This is the accepted version of the following article:
DEMERS-POTVIN, A.V. & LARSSON, H.C.E. (2019) Palaeoclimatic reconstruction for a Cenomanian-aged angiosperm flora near Schefferville, Labrador. Palaeontology, 62, 1027-1048. https://doi.org/10.1111/pala.12444

Palaeoclimatic reconstruction for a Cenomanian-aged angiosperm flora near Schefferville, Labrador

by ALEXANDRE V. DEMERS-POTVIN[1,2]* *and* HANS C.E. LARSSON[1,2]

[1]Department of Biology, McGill University, 1205 Dr Penfield Ave, Montreal, QC, Canada;

[2]Redpath Museum, McGill University, 859 Sherbrooke Street W., Montreal, QC, Canada;

e-mails: alexandre.demers-potvin@mail.mcgill.ca; hans.ce.larsson@mcgill.ca

*Corresponding author

ABSTRACT

An understanding of local and regional climate trends is essential to investigate the remarkable angiosperm radiation that happened during the Albian-Cenomanian transition. However, many of the inland depositional environments pioneered by the first modern angiosperms are poorly represented in the fossil record. Eastern Canada in particular has a very poor Mesozoic record. In this paper, we present the first multivariate palaeoclimate analysis (CLAMP) for the environment of a geologically isolated woody dicot dominated flora found in the Redmond no.1 mine, Labrador, near Schefferville, with an estimated Cenomanian age. It reveals that the Redmond flora would have experienced a mean annual temperature of 15.1 ± 2.1 °C, one of the coolest recorded for North America at this time. These results confer the Redmond no.1 site a warm temperate and fully humid climate with a hot summer, in accordance with previous qualitative palaeoclimate estimates. This flora fits smoothly into palaeolatitudinal MAT gradients that use other Cenomanian-estimated North American floras. Despite an inland setting, the climate analysis does not recover a significantly higher degree of seasonality than the sites to which it is compared, which agrees with established climate equability models for the Cretaceous and Paleogene. This study also introduces 15 new morphotypes discovered in recent fieldwork. The eventual description of the species they represent may refine our dating estimates for the Redmond Formation. A greater understanding of the depositional environment and of the natural history of these angiosperms is required to improve this community's characterization, along with estimates from other proxies.

Key words: angiosperms, Cenomanian, palaeoclimate, MAT, Redmond Formation

The Albian-Cenomanian transition in the middle of the Cretaceous period witnessed ecological and evolutionary changes that laid the foundations of modern terrestrial communities. Not least of these is the radiation of the angiosperms from the disturbed or early successional settings that had witnessed their evolution for the previous 30 Myr (Doyle and Hickey 1977; Crane *et al.* 1995). After thriving as lowland riparian and estuarine weeds (Royer *et al.* 2010), early angiosperms underwent a spectacular ecological diversification and expanded their geographical range into more stable inland environments, often coinciding with the decline of established groups such as conifers, pteridophytes, ginkgoaleans and Benettitales (Retallack and Dilcher 1986; Lupia *et al.* 2000; Coiffard *et al.* 2012).

Many of the hypotheses that attempt to explain this floral turnover revolve around a combination of biotic and abiotic factors. In certain modern environments, angiosperms are known to have a higher competitive ability than other plants due to higher productivity under high nutrient concentrations (Berendse and Scheffer 2009). This competitive ability may have led to positive feedbacks with increased fire regimes during the Albian-Cenomanian transition as global atmospheric pCO_2 and temperatures increased (Bond and Scott 2010). These abiotic changes may also have induced a positive feedback with photosynthetic capacity through an increase in venation complexity, which is correlated with an increase in wood hydraulic efficiency and the appearance of the first angiosperm trees (Philippe *et al.* 2008; Feild *et al.* 2011). This remarkable radiation can be explained in part by co-evolution with pollinating insects such as Hymenoptera and Lepidoptera (Grimaldi 1999), but also by an understanding of global and regional climatic trends. The latter can be detected in the foliar physiognomy.

Despite a constant flow of newly described palaeofloras from across the world, some regions, such as eastern Canada, remain poorly represented in the fossil record. The southern half of the palaeocontinent of Appalachia is well represented by coastal and estuarine floras ranging in time from the Barremian to the Cenomanian (Newberry 1886; MacNeal 1958; Doyle and Hickey 1977), and changes from the Albian to the Turonian are represented by floras from the western coast of Laramidia (Miller *et al.* 2006; Jonsson and Hebda 2015). In comparison, very little is known of Appalachia's northern inland ecosystems. Early palaeolatitudinal climate gradients established for Cenomanian North America were almost totally restricted to low palaeolatitudes around 30°N (Wolfe and Upchurch 1987), though updated gradients are complemented by recently studied floras from Alaska (Spicer and Herman 2010).

An enigmatic angiosperm-dominated flora from Labrador may provide insight into this poorly studied part of the Cretaceous world. Soon after its discovery alongside a few insect impression fossils during iron ore prospection near Schefferville, it was biostratigraphically correlated with North American Cenomanian-aged floras, though no detailed description was ever published (Dorf 1959, 1967). So far, no other Mesozoic angiosperm floras have been reported from eastern Canada. This would also make it one of the earliest known woody dicot floras to flourish far inland, alongside assemblages from central Alaska's Yukon-Koyukuk basin (Herman *et al.* 2016), Siberia's Vilui basin (Spicer *et al.* 2008), and the Winton Formation of central-western Queensland (Fletcher *et al.* 2014). A quantitative palaeoclimate estimate using leaf margin analysis (LMA) has already been obtained for the Labrador flora and was compared with coeval floras to the North and South (Armstrong 1993; Miller *et al.* 2006). However, this univariate method

for palaeoclimatic reconstruction is fraught with limitations (Greenwood *et al.* 2004; Peppe *et al.* 2011; Li *et al.* 2016), and estimates from this site have been based on a limited dataset.

In this paper, we present the first palaeoclimatic reconstruction founded on the Climate Leaf Analysis Multivariate Program (CLAMP) (Wolfe 1993; Spicer 2006) for this locality. The morphological diversity of the flora under study has also been expanded by the recent discovery of new leaf morphotypes on the field. These results are integrated to data from approximately coeval Cenomanian North American floras and refine our understanding of climatic trends at this ecosystem's local scale and at a broader continental scale.

GEOLOGICAL SETTING OF THE LABRADOR CRETACEOUS FLORA

The angiosperm flora that is the object of this study is preserved in the Redmond Formation, a sedimentary unit named after the Redmond no.1 mine, located 16 km south-southeast of Schefferville (Dorf 1967) at a latitude of 54°41'N and a longitude of 66°45'W, close to the Quebec border (Fig. 1). This abandoned iron mine contains the only known exposure of the formation in a very complex geological setting. It contains clastic minerals constituting three distinct lithologies, although almost all fossils have been found in a single one: a fine-grained, evenly banded ferruginous argillite with a very pronounced umber colour and a 60% red hematite content (Blais 1959). Before iron ore mining operations brought the formation out of stratigraphical context, it formed a very restricted bed not exceeding 1.5 m in thickness, traced for approximately 152 m (Blais 1959). This bed was lying in the upper section of a basin-shaped space 1,524 m long, 508

m wide, and up to 183 m deep containing sterile argillite and iron-rich 'rubble ores', which was in turn overlain by a 3 to 5-m overburden of glacial deposits (Dorf 1967; Séguin 1971). The argillite in the thin bed has a finer grain size, a darker colour, and a much higher abundance of well-preserved fossils, than the surrounding sterile argillite.

Hypotheses concerning the depositional environment of these fossils have yet to be tested. The most widely accepted one proposes a shallow lacustrine setting based on very fine grain size, a very thin lamination, and well-preserved soft tissues such as leaf and wing venation in fossilized plants and insects (Blais and McMahon 1958; Blais 1959). These characteristics distinguish low-energy freshwater systems such as lakes from higher-energy fluvial/deltaic systems in which soft-bodied organisms are more likely to be decomposed (Behrensmeyer and Hook 1992, pp.42-43). Blais (1959) states that the high alumina content displayed in the argillite is indicative of a lateritic palaeosol, a soil type usually formed in tropical to subtropical climates (Craggs *et al.* 2012), although this evidence alone is barely sufficient to suggest a hypothesis. Historical fossil collections for the site contain angiosperms leaves representing at least 27 species, which are the main focus of this study, along with at least 1 lycopod, at least 4 true fern species (spread among Polypodiales and Gleicheniales), and at least 4 conifer species (Dorf 1959, 1967; Armstrong 1993; Fig. 2). Along with an assortment of insect species (Carpenter 1967; Emerson 1967; Ponomarenko 1969; Rice 1969; Fig. 3), these fossils offer a glimpse of a lakeshore environment surrounded by an angiosperm-dominated mixed mesophytic forest.

The Redmond basin is underlain disconformably by stratified iron ores found in jaspoid and carbonate-silicate cherts that are part of the iron-rich Sokoman Formation,

deposited around 1,878 MA in the Paleoproterozoic (Conliffe 2016). The Sokoman is underlain by the Ruth Formation, composed of ferruginous shale (Blais 1957, 1959). Together, they are part of the Kaniapiskau Supergroup, the geological unit that constitutes the Labrador Trough, a 48-km wide folded and faulted geosyncline containing sedimentary and volcanic rocks that stretches for approximately 1,120 km along the border of northeastern Quebec and western Labrador (Blais 1957; Zajac 1974; Conliffe 2016), and along the eastern margin of the Archaean Superior Province (Conliffe *et al.* 2012).

The Labrador Trough has been formed by two main orogenic events : a period of folding in the late Precambrian (between 1,500 and 1,250 MA), and a later one for much of the Mesozoic that probably led to the opening of the North Atlantic ocean between 250 and 200 MA (Tremblay *et al.* 2013; Conliffe 2016). The Redmond basin is likely the remnant of a graben: this folding and down-faulting continued after the deposition of the Redmond fossiliferous argillite bed giving its steep dip of 45° to the east (Blais 1959). As this tectonic activity increased the graben's depth, it was progressively infilled with muddy sediments containing dead leaves and insects (in the case of the Redmond Formation), and/or rubble ores of clastic origin mixed with fallen trees (Blais and McMahon 1958). Similar basins were reported in the French, Burnt Creek and Ruth Lake mines, located 4 km West of Schefferville. In Ruth Lake, entire lignitized tree stumps were found in a breccia 30 m below ground surface, some of which reach almost 1 m in diameter (Usher 1954). Nowadays, they are also out of context because of the mining activities that followed their discovery.

The presence of a megafloral assemblage in the ferruginous argillite bed provides the only relative dating estimate for the Redmond Formation itself. Dorf (1959) conducted a biostratigraphical correlation with already known North American floras and found that it was most similar in composition to the Raritan, Dakota, and Tuscaloosa formations, which are all considered of Cenomanian age, between 93.9 and 100.5 MA (ICS Chronostratigraphic Chart, v 2018/8; Fig.1).

Based on the interbedding between the clays and the rubble ores, Blais (1959) concluded that the latter must have been of similar age (Late Cretaceous) and included them in the Redmond Formation. Assuming its dating is correct, this makes it the only known exposure from the Mesozoic era in the Quebec/Labrador Peninsula. The sedimentary unit in closest spatial and temporal proximity would be northern Ontario's Albian Mattagami Formation (White *et al.* 2000).

While the age of the argillite formation is already poorly constrained, that of the surrounding rubble ores is even more debatable. The interbedding noted by Blais (1959) only proves that some of the leaching happened during the Cretaceous (Conliffe *et al.* 2012; Conliffe 2016). The implied long duration of fault movement and resulting rubble ore formation restrains us from including the entirety of the region's rubble ores in the Redmond Formation (*contra* Blais, 1959). This makes it impossible to correlate the Ruth Lake wood to the insects and leaves found in the Redmond no.1 mine's ferruginous argillite, and so renders the tree stumps' cell structure unsuitable as an alternative palaeoclimate proxy (Carlquist 1977; Wolfe and Upchurch 1987) for Cenomanian eastern Canada.

MATERIAL AND METHODS

Fossil collection and identification

The fossils used in this study were collected from the Redmond no.1 mine over five separate occasions: the first in September 1958 for Princeton University (Dorf 1959; Rice 1969), which now resides at the Yale Peabody Museum of Natural History (YPM) ; two for the Geological Survey of Canada (GSC) (G. Gross, 1960 and D.C. McGregor, 1961); one in 2013 by the *Musée de paléontologie et de l'évolution* (MPE); and a joint expedition between the MPE and the Redpath Museum (RM) in August 2018, in which the first author participated. On the 2013 and 2018 expeditions, the fossils were surface collected on spoil piles scattered around the now flooded mine since the original bed had long been destroyed by mining activities. Alongside new leaf specimens, new insects were discovered, including the first aquatic nymphs reported from the site, as well as more complete aquatic coleopteran specimens (Figs 3A, 3C; Demers-Potvin and Larsson, in prep.). The 2013 expedition also produced ichnofossils of bioturbators moving along the water bottom (Fig. 3F). A survey of neighbouring mines in 2018 did not reveal any exposed fossil-bearing argillites similar to those found in the Redmond no.1 mine.

The YPM collection is the only one in which an attempt to identify the flora was made before this study. Its classification was undertaken by Leo J. Hickey; the notes he left with the YPM specimens were consulted by the first author to guide our subsequent identifications. A total of 177 specimens have been assigned to 46 morphotypes using leaf architectural characters (Hickey 1973; Ellis *et al.* 2009). The identification of most of the morphotypes in this study agrees with the species identifications originally performed by Hickey. However, 15 morphotypes are based on new leaf forms discovered in the

2013 and 2018 expeditions, and one is based on a specimen observed at the GSC (Demers-Potvin and Larsson 2019). Each has been assigned a morphotype quality index (MQI), ranging from 0 to 7, that expresses the completeness of the specimens on which it is founded (see Harris and Arens 2016 for details). The argillite tends to fracture conchoidally, which means that leaves found along bedding planes are often fragmentary. The ensuing loss of morphological characters introduces much uncertainty in the attribution of a specimen to a given morphotype. For this reason, many of the leaf fragments collected could not be integrated into the analysis.

A summary of the morphotypes is presented in Table 1. Photographs of the morphotype exemplars are presented in Figs 4-7. GSC, MPE and RM specimens were photographed with a Sony a6000 camera with an FE2.8/50 macro lens, and YPM specimens with a Nikon D7100 camera with a 50mm macro lens. Measurements used in the descriptions were made on Fiji (Schindelin *et al.* 2012). More complete descriptions are found in Demers-Potvin and Larsson (2019).

Palaeoclimatic Reconstruction

One way of estimating a palaeoecosystem's climate using biological proxies is to infer it from the physiognomy of its fossil leaves. A positive correlation in many extant floras between the percentage of species with untoothed margins and their habitat's mean annual temperature (MAT) was first proposed by Bailey & Sinnott (1915, 1916), and later became the basis for the univariate method of leaf margin analysis (LMA) (Wolfe 1979; Wing and Greenwood 1993; Wilf 1997; Greenwood 2007). Based on the observation that leaf physiognomy responds to multiple environmental factors (Dolph

and Dilcher 1979), a more complex palaeoclimate reconstruction model, the Climate Leaf Analysis Multivariate Program (CLAMP), was developed by Wolfe (1993) and subsequently refined (e.g. Spicer 2006; Yang *et al.* 2015). This is the first time that the Redmond flora's climate has been estimated with this method. Every CLAMP analysis on a fossil assemblage is based on two spatially related modern datasets. The first is a physiognomic calibration dataset composed of extant floras from sites worldwide that have been scored for the same character states as fossil sites. Every physiognomic calibration dataset has its corresponding meteorological calibration dataset in which, in the most common configuration, 11 climate parameters found to be correlated with leaf physiognomy have been measured on each site or derived from standard global gridded data. The data from physiognomic and meteorological dataset matrices is united in a Canonical Correspondence Analysis (CCA) (ter Braak 1986). The morphotypes of a given fossil site are then scored using the same protocol as the modern sites. This positions a fossil leaf assemblage passively in the physiognomic space formed by leaves from extant calibration vegetation, leading to quantitative predictions of palaeoclimate parameters at the time of fossil deposition. Further details on the method can be found on the CLAMP website (Spicer 2006; Yang *et al.* 2011, 2015).

To ensure a sufficiently high statistical precision for the results, a minimum of 20 fossil morphotypes (Wolfe 1993), with a scoring completeness greater than 66% (Yang *et al.* 2011), is recommended. After its 46 morphotypes were scored, the Redmond flora displayed a CLAMP scoring completeness of 65% (see scoresheet in Demers-Potvin and Larsson (2019)). The matrix was analyzed using the CLAMP Online tool (Spicer, 2006, accessed September 27 2018; Yang et al., 2011). A preliminary CLAMP analysis was

made using global calibration files (PhysgGlobal378 and HiResGRIDMetGlobal378, n = 378 sites), which positioned the Redmond flora well away from sites in cold climates (Spicer 2006). Extraneous evidence of an environment that did not experience a freezing period comes from the occurrence of an entomofauna in which some taxa are predominantly associated with tropical to subtropical climates, such as a medium-sized phasmatodean (Rice 1969; Brock 2004, p.222; Fig. 3B), a termite (Emerson 1967; Grimaldi and Engel 2005, p.241; Fig. 3D), and a snakefly belonging to the extinct family Alloraphidiidae (Carpenter 1967; Grimaldi and Engel 2005, p.339; Fig. 3E).

A more definitive analysis was performed using the Physg3brcAZ calibration dataset derived from temperate Northern Hemisphere sites (n = 144). Climate calibrations were made using both the gridded (GRIDMet3brAZ) and ungridded (Met3brAZ) meteorological datasets to compare results between the two sampling methods. While the ungridded dataset is based on calibration vegetation sites, the gridded dataset attempts to correct for the lack of climate stations close to potential calibration vegetation sites at low latitudes by using a 0.5° x 0.5° grid of global interpolated climate data based on the dataset of New *et al*. (1999) (Spicer *et al.* 2009).

RESULTS

The CLAMP results for the Redmond no.1 site are presented in Table 2. The first CLAMP analysis for this locality presents a MAT of 15.1 ± 2.1 °C. The results from gridded and ungridded datasets are statistically indistinguishable, in accordance with Spicer *et al*.'s (2009) tests.

Not only does the palaeoclimate data from the Redmond flora yield invaluable information on the environment of a region otherwise devoid of Cretaceous fossils, but the site would have occupied a palaeolatitude estimated at 48.8°N (van Hinsbergen *et al.* 2015*a*; Table 3). This means it is the most northerly site from eastern North America to present an early Late Cretaceous angiosperm flora, since the age of Greenland's Atane Formation is questionable (Wolfe and Upchurch 1987; Boyd 1993). This palaeolatitude is poorly represented in the eastern North American Cenomanian angiosperm fossil record (Miller *et al.* 2006). The climate parameter values of the Redmond no.1 site were then compared with coeval North American Cenomanian floras (Table 3). Comparative mean annual temperature values from leaf-margin analysis (LMAT) were obtained from entire-margin frequencies of 12 sites compiled by Miller *et al*. (2006). The original LMAT estimates for the Redmond Formation were calculated by Hickey & Armstrong (1998), those for the Raritan, Patapsco, Dakota, Woodbine and Dunvegan formations were calculated by Wolfe and Upchurch (1987), and that of Chandler, Alaska, was calculated by Parrish and Spicer (1988).

Comparative CLAMP values were obtained from GRIDMET3BR analyses of three sites: Tuscaloosa, Woodbine (Spicer and Herman 2010), and Nanushuk (Herman *et al.* 2016). Additionally, two floras from the Dakota Group (age Cenomanian) were scored for CLAMP estimates (see Methods) to increase the Cenomanian site sample size. One of these floras was collected in Fort Harker, Ellsworth Co., Kansas, during separate expeditions (Lesquereux 1892), and is now curated at the Yale Peabody Museum of Natural History (YPM). After examination, it was divided into 92 morphotypes with 89% completeness. The other, found in Rose Creek, Jefferson Co., Nebraska, was scored from

published descriptions (Upchurch and Dilcher 1990) into 18 morphotypes with 68% completeness. The CLAMP scoresheets for these additional floras are provided in Demers-Potvin and Larsson (2019).

The MAT data from Table 3 was then plotted against palaeolatitude with separate regressions for the LMA and CLAMP estimates on Fig. 8. For each site, palaeolatitude estimates were obtained from van Hinsbergen *et al*. (2015*a*), using the reference frame of Torsvik *et al*. (2012) (see van Hinsbergen *et al*. (2015*b*) for more details). We still deem the LMA-based implied regression a necessary comparison because it is based on a larger sample size than the CLAMP-based regression. The R^2 values and regression equations are presented in the legend to Fig. 8.

DISCUSSION

The dominance of medium-sized angiosperm leaves in the Redmond assemblage, as well as the presence of insect taxa accustomed to mild or warm climates, led to qualitative hypotheses predicting a warm temperate to subtropical climate (Blais 1959; Dorf 1959). According to the updated Köppen-Geiger climate classification system (Kottek *et al.* 2006), the region's coldest month mean temperature (CMMT) of 7.8 ± 3.4°C is between the -3°C and 18°C values that define warm temperate climates, its disparity in precipitation between the three wettest and three driest months is nonsignificant, and its warm month mean temperature (WMMT) exceeds 22°C. A marked disparity of more than 15°C between CMMT and WMMT, along with a growing season of 8.4 ± 1.1 months, is indicative of a moderate seasonality. The growing season would have been far longer than that of more extreme environments such as Late

Cretaceous Alaska's polar deciduous forests (Herman *et al.* 2016), which is not surprising considering the Redmond Formation's intermediate palaeolatitude and coincidentally long photoperiod. These quantitative results confer the Redmond no.1 site a warm temperate and fully humid climate with a hot summer (Cfa) (Kottek *et al.* 2006), which confirms the initial qualitative hypotheses. This precision in climate classification was attained in part because of the multivariate nature of CLAMP.

Contrary to the LMA used in previous work on the Redmond Formation (Armstrong 1993; Hickey and Armstrong 1998), CLAMP encompasses 12 more leaf physiognomic characters that demonstrate a response to climate parameters. These additional variables provide more insight into an extinct ecosystem's seasonal cycle and photoperiod (Herman *et al.* 2016). By acknowledging the covariation between many leaf traits and multiple environmental factors (Dolph and Dilcher 1979), CLAMP assumes that a climate signal can be obtained from more correlations than the single correlation on which LMA is founded (Wolfe 1993; Spicer 2006; Yang *et al.* 2015). Conversely, leaf margin analyses of floras found in freshwater settings (the most common depositional environment) are more susceptible to confounding factors such as soil hydrology (Kowalski and Dilcher 2003), overrepresentation of toothed-margined species in riparian settings (Burnham *et al.* 2001) and evolutionary history (Greenwood *et al.* 2004; Little *et al.* 2010; Peppe *et al.* 2011). CLAMP also has an advantage over climate analysis methods based on more continuous leaf character states, such as Digital leaf physiognomy (Royer *et al.* 2005; Greenwood 2007; Peppe *et al.* 2011), since it has been thoroughly tested for a longer time, and its uncertainties better addressed and understood (Wolfe 1993; Spicer 2006; Yang *et al.* 2015). Despite the fact that a single character (leaf

margin) still explains >80% of the variance in MAT (Wing and Greenwood 1993; Wilf 1997), the CLAMP results from the gridded dataset remain the most accurate ever produced for the Redmond flora.

Sampling uncertainties. The completeness score of the Redmond flora is just below the recommended threshold of 66%, so information loss for some characters may affect the results. The fragmentary nature of many of the new morphotypes – often represented by only one RM specimen – takes a particular toll on the completeness of the dataset. When they are removed, it rises to 80%. Unsurprisingly, the morphotypes with the highest sample size (8 and 26) are also those that display the highest phenotypic plasticity (Figs. 4I-L, 6D-F; Demers-Potvin and Larsson 2019). Conversely, the small sample size of most morphotypes (91.3% represented by fewer than 10 specimens; see Table 1) means that much of the phenotypic plasticity characteristic of Cenomanian floras is not detected in the fossil assemblage (Spicer, pers. comm., 2019), which may lead to over-splitting of morphotypes in the presence of newly acquired specimens with new morphological character combinations. It has been demonstrated that incomplete preservation has a particularly detrimental effect on the accuracy of palaeoclimate estimates derived from sites with many singletons (Royer *et al.* 2005), as is the case for the Redmond flora (Table 1). At least, the high number of singletons leads to a morphotype diversity that is much higher than the recommended minimum (see Methods). Demers-Potvin and Larsson (2019) discuss the erection of these new morphotypes, but a more detailed description of potentially new species is necessary to resolve their status.

Another sampling uncertainty has biological ramifications for the climate predictions. It is assumed in this study that all angiosperm leaves recovered are indeed woody dicots (Dorf 1959, 1967). Hickey and Armstrong (1993) classified YPM specimens of very small size in this guild, and so the classification of morphotypes discovered in more recent expeditions maintained this consistency. Herbaceous plants have been shown to display much less consistent physiognomic responses to climate (Li *et al.* 2016), but their effect on our results are probably trivial, because their leaves do not shed, and so rarely fossilize. In turn, this statement assumes that Late Cretaceous lacustrine palaeofloras are sufficiently similar to modern ones.

In any case, the more taxon-dependent data supports the woody dicotyledonous nature of this flora. Table 1, Figs 4-7 and Demers-Potvin and Larsson (2019) show that many of these morphotypes can reach a notophyll size class and a complex venation pattern, which are characteristic of woody dicots. Many are comparable in size and complexity to newly discovered leaves from the Turonian Mancos Shale Formation which have been attributed to trees (Jud *et al.* 2018). This would make the Redmond flora slightly older, assuming the relative dating of the formation is accurate (see Geological setting).

Taxon-independent leaf economic traits could also be determined. One such trait is vein density (D_v), which has been shown to reflect life-form in angiosperm leaf assemblages (Crifò *et al.* 2014) and could be quantified on a much larger sample size. Leaves with a higher D_v have an improved photosynthetic capacity, and their synchronous appearance with the oldest angiosperm wood known suggests that it was a key adaptation to the increase in hydraulic capacity necessary to sustain such complex

organisms as trees (Philippe *et al.* 2008; Feild *et al.* 2011). This study should be the next step to improve the ecological characterization of each species of the Redmond flora, refining our capacity to build subsequent CLAMP datasets. Most importantly, its results could support Dorf's (1959, 1967) hypothesis that the larger Redmond leaves belong to some of the oldest known angiosperm trees.

Local spatial and temporal resolution. Blais' (1959) description of the Redmond Formation in geological context is highly valuable, since it is the only way for modern workers to gain insight into the site's geological setting. Furthermore, the hypothesis of a lacustrine depositional environment is now confirmed after the discovery of the first articulated and relatively complete specimens of aquatic insects (Figs 3A, 3C; Demers-Potvin and Larsson, in prep.). The argillite's fine grain size and thin laminations were already indicative of a lake environment (Picard and High 1972), and so is the remarkable preservation state of some of the newly discovered insects (Grimaldi and Engel 2005, p.42).

However, Blais' survey did not address the site's temporal resolution since it did not approach it from a palaeoecological perspective. The formation's modest depth of 1.5 m (Blais 1959) and its lacustrine origin suggest a high temporal resolution (Behrensmeyer and Hook 1992, pp.82-83). Unfortunately, Blais did not calculate sedimentation rates based on its laminations, nor did he map fossil occurrences along a stratigraphic section, to support his hypothesis. If such a section had been produced, it might have been possible to infer the lake's variations in oxygen content, which could have been inferred by mapping the occurrences of ichnofossils produced by benthic

bioturbators (Behrensmeyer and Hook 1992, pp.42-50). In turn, insight on oxygen content could have contributed to an explanation of the fauna and flora's preservation state. It is mentioned that the bed was evenly laminated, but it remains difficult to estimate the duration represented by each lamination in this argillite. As for the distribution of the flora along the temporal axis of the formation, it is not specified whether plants were concentrated at a few levels, or widespread along the entire stratigraphic column (Dorf 1967). This means that any palaeoclimate estimate derived from this flora must account for some taphonomic time-averaging. Further sedimentological analyses of these argillite laminations, as well as a refinement of the current relative dating estimate based on the description of new macrofossils and palynological analyses, may provide insight on this issue.

As for the spatial resolution, it is quite difficult to assess, since most of the leaves found in the fossil assemblage could have belonged to trees growing away from the lake's vicinity (Greenwood 1992). At least, the specimen that represents Morphotype 46 might be of a more autochthonous origin (Fig. 6O; Demers-Potvin and Larsson 2019) . This leaf displaying a peltate petiole origin is very similar to leaves from the Potomac Group that were proposed to be floating on the water surface, a substrate where there is less mechanical stress on the petiole (Hickey and Doyle 1977). On the other hand, a peltate petiole origin is also encountered in leaves growing from tropical forest trees (Jacques *et al.* 2015). Since its habitat is not certain and its morphotype quality is among the highest (Table 1), we have decided to include it in the CLAMP analysis along with other morphotypes whose woody dicotyledonous status is less equivocal.

The Cenomanian Quebec/Labrador climate in a North American context

The Redmond MAT is the coolest recorded for Albian-Cenomanian eastern North America, and likely attributable to the combination of a higher latitude than other known sites and an inland location. Such conditions have been reported elsewhere at this time (Spicer *et al.* 2008; Herman *et al.* 2016). Complementary CLAMP results suggest a moderate seasonality in the Redmond flora's inland setting (Table 3), though it certainly was not as high as Armstrong (1993) imagined: neither the length of the growing season (LGS) nor the disparity between CMMT and WMMT are significantly different from the other sites it was compared with. The MAT gradient suggests either a genuine climatic equability between inland and nearshore environments in Cenomanian eastern Canada, or locally mild riparian conditions favourable to angiosperm invasion, or both. Given the global warming that was occurring during the Albian-Cenomanian transition, the latter hypothesis must be considered (Arens and Harris 2015), although it can only be tested with the discovery of more exposures of the Redmond Formation in Quebec and Labrador. In any case, the probable woody dicot life-form of most morphotypes indicates that they could thrive in more stable environments alongside gymnosperms by the Cenomanian, which is consistent with the floral composition of approximately coeval assemblages (Spicer and Herman 2001; Spicer *et al.* 2002).

For the moment, it is more parsimonious to argue that the data agrees broadly with a trend of continental sites showing a much more equable seasonal range of temperatures in the Cretaceous and Paleogene than in the present (Wing and Greenwood 1993; Spicer *et al.* 2008). In the Cretaceous, North America was rotated clockwise so that the western landmass of Laramidia was situated further north (Spicer and Herman 2010;

Bamforth *et al.* 2014; Herman *et al.* 2016) and the eastern landmass of Appalachia (of which the Quebec/Labrador Peninsula constituted the northern extremity) was situated further south. It is no surprise, then, that a site that had a lower palaeolatitude in the Cretaceous than today, coupled with a far more equable MAT gradient, had such a mild climate with a long photoperiod that supported such a luxuriant flora.

The gradient derived from Miller *et al*. (2006) using LMA has a markedly steeper slope than that derived from CLAMP (Fig. 8). In light of the previous discussion, the larger sampling biases associated with LMA seem to lead to a less equable climate gradient model. Not only do MAT estimates seem more accurate with CLAMP than with LMA at the local scale, but they seem more precise at the regional scale and provide additional information about seasonality and photoperiod.

Limitations of regional to global palaeoclimate studies. The Albian-Cenomanian transition is probably the earliest time in geological history to be suitable for palaeoclimate analyses based on CLAMP and LMA, since it witnesses the advent of the few angiosperm life-forms to show a relationship between leaf physiognomy and climate parameters (Lupia *et al.* 2000; Feild *et al.* 2011). No wonder it is accurate only for sites less than 100 Myr old (Wolfe 1993; Spicer 2006). This implies that results for a flora that probably existed very close to this time limit must be interpreted with caution.

Since CLAMP assumes that the physiognomic response of leaves to climate has not significantly changed for 100 Myr, it has been suggested to be more difficult to apply confidently to older assemblages (Peppe *et al.* 2011). This could be a particular problem for assemblages representing ecosystems without any modern analogue, such as the

Cretaceous polar mixed deciduous forests of Alaska (Spicer and Herman 2010; Herman *et al.* 2016). Furthermore, Albian-Aptian species that have a similar morphology to Late Cretaceous woody dicotyledons (Hickey and Doyle 1977) were long considered too evolutionarily distant to have a similar physiognomic response to climate, despite evolving under the same physical and mechanical constraints as modern leaves. Since the Cenomanian was a time of rapid global warming, early woody dicots were thought to be largely experimental forms that could not be assumed to behave similarly to modern forms (Spicer and Parrish 1986). If the physiognomic response of Cenomanian leaves to climate displayed a strong phylogenetic signal, a better understanding of these species' evolutionary history could help alleviate the uncertainties in 'taxon-independent' methods such as CLAMP (Little *et al.* 2010). However, many genera from this time interval display phenotypic plasticity, which could blur the phylogenetic signal. This phenomenon is observed in at least two of the Redmond flora's morphotypes (Figs. 4I-L, 6D-F; Demers-Potvin and Larsson 2019; Spicer, pers. comm., 2019).

Since this assumption was made, however, many more fossil assemblages have been scored with CLAMP, and none of the Albian-Cenomanian floras (including the Redmond flora) have plotted outside the modern calibration space to suggest a significant change in the climate-physigonomy relationship (e.g. Fletcher *et al.* 2014; Arens and Harris 2015). Furthermore, a global study of the 378 CLAMP sites has demonstrated that biogeographic history has little effect on the observed correlations between leaf form and climate (Yang *et al.* 2015). In light of these considerations, the validity of the Redmond flora for palaeoclimate estimates should be further assessed by a more formal taxonomic description of the new species present among the morphotypes recognized in this study.

This constraint leads to another, where Cenomanian angiosperm sites with a diversity of woody dicot morphotypes sufficient for CLAMP scoring are rare, as is the case in North America (Wolfe and Upchurch 1987; Miller *et al.* 2006). This inevitably leads to systematic time-averaging of different sites, for instance in the case of our palaeolatitudinal MAT gradient. Since the global climate in the Cenomanian was changing quite rapidly, and since many of the sites used (such as Redmond no.1) have a very poor stratigraphic control, a gradient for this age contains especially large uncertainties. In this regard, the discovery and scoring of new palaeofloras (Jud *et al.* 2018) remains an essential aspect of palaeoclimatology based on biological proxies.

CONCLUSIONS

This is the first palaeoclimate estimate for the environment of the Redmond flora to use a multivariate method (CLAMP). At the local scale, its results confirm previous hypotheses according to which 'early' Late Cretaceous Quebec/Labrador would have experienced a mesothermal humid climate with a hot summer and offer a small glimpse of an environment that – to our knowledge – has been very sparsely preserved in the fossil record. Together, they contribute significantly to our understanding of Cretaceous eastern Canada, in the hope of refining the testing of hypotheses on the angiosperms' remarkable radiation.

The CLAMP results support a general Cretaceous and Paleogene trend of inland environments having a climate as equable as that of coastal environments. However, such comparisons at the regional to global scale with sites from the same age bin with poor stratigraphic control must be treated cautiously, since they can lead to systematic time-

averaging that confounds observed palaeolatitudinal climate trends. This is especially concerning for periods of rapid climate change such as the Albian-Cenomanian transition, and it leads us to favour the detection of such climate trends at a more local scale to gain more insight on the radiation of the angiosperms. We acknowledge that the Redmond Formation does not have an ideal geological setting to support palaeoecological investigations, which is regrettable considering the scientific importance of one of the oldest inland angiosperm floras known. The Labrador Trough must be prospected further in the hope that more of this mysterious palaeoecosystem can be revealed.

Beyond palaeoclimate estimates, this study also contributed to an expansion of the morphological angiosperm diversity from the Redmond no.1 site, with the addition of 16 new morphotypes. Their formal description is essential: a more complete flora (complemented by an eventual study of the palynoflora) refines biostratigraphical correlations to estimate its age, and some species may increase broad-leafed tree diversity in the fossil record at a time in which they were radiating. The ecological characterization of the community must also be refined, either by studying leaf economic traits such as leaf vein density to gain insight on many morphotypes' life-forms, or by increasing our understanding of this flora's depositional environment. In turn, this will define much more clearly the assemblage that can be tested in future palaeoclimate estimates based on biological proxies. An estimate from an alternative geochemical proxy, such as clay weathering, could also support the study that has been presented here.

Acknowledgements. The authors wish to thank M. Cournoyer for providing access to the *Musée de paléontologie et de l'évolution*'s (MPE) collections at the very start of this

project, and who accompanied the first author in the field in August 2018. Thanks are extended to N. Sheppard and M. Chartier for their assistance in this fieldwork, and to the McGill Subarctic Research Station in Schefferville, QC, for the accommodation it provided. We also thank A. Howell for providing Redpath Museum (RM) accession numbers to recently collected specimens on such short notice. As for specimens examined during research travels, S. Hu is graciously thanked for providing access to the paleobotany collections at the Yale Peabody Museum of Natural History (YPM), as well as S. Butts and J. Utrup for providing access to the YPM's invertebrate palaeontology collections, and M. Coyne for providing access to the Geological Survey of Canada (GSC) collections. We acknowledge the contributions of J.-P. Guilbault, P. Bédard and J. Letendre for their initial collection efforts for the MPE alongside M. Cournoyer at the Redmond no.1 mine back in 2013. Finally, the authors wish to thank the editors, B. Lomax and S. Thomas, as well as R. Spicer, D. Greenwood and E. Bamforth for improving this paper with their reviews. This research was supported by funding from the *Fonds de recherche Nature et technologies Québec* (FRQNT), a National Geographic Society Early Career Grant, the Northern Scientific Training Program (NSTP), a Redpath Museum Class of 66 Award, and the Canada research chair to HCEL.

DATA ARCHIVING STATEMENT

Data for this study (including CLAMP scoresheets and a morphotype catalogue) are available in the Dryad Digital Repository: https://datadryad.org/review?doi=doi:10.5061/dryad.bg7pd54 **[please note that the data**

for this paper are not yet published and this temporary link should not be shared without the express permission of the authors]

REFERENCES

ARENS, N. C. and HARRIS, E. B. 2015. Paleoclimatic reconstruction for the Albian-Cenomanian transition based on a dominantly angiosperm flora from the Cedar Mountain Formation, Utah, USA. *Cretaceous Research*, **53**, 140–152.

ARMSTRONG, T. B. 1993. A Palaeoclimatic Interpretation of a Cenomanian Inland Flora from Schefferville, Quebec, Canada.Unpublished Senior Thesis, Yale University, 108pp.

BAILEY, I. W. and SINNOTT, E. W. 1915. A Botanical Index of Cretaceous and Tertiary Climates. *Science*, **41**, 831–834.

——— and ———. 1916. The Climatic Distribution of Certain Types of Angiosperm Leaves. *American Journal of Botany*, **3**, 24–39.

BAMFORTH, E. L., BUTTON, C. L. and LARSSON, H. C. E. 2014. Paleoclimate estimates and fire ecology immediately prior to the end-Cretaceous mass extinction in the Frenchman Formation (66 Ma), Saskatchewan, Canada. *Palaeogeography Palaeoclimatology Palaeoecology*, **401**, 96–110.

BEHRENSMEYER, A. K. and HOOK, R. W. 1992. Paleoenvironmental Contexts and Taphonomic Modes. *In* BEHRENSMEYER, A. K., DAMUTH, J. D., DIMICHELE, W. A., POTTS, R., SUES, H.-D. and WING, S. L. (eds.) *Terrestrial Ecosystems through Time*, The University of Chicago Press, Chicago, 121 pp.

BERENDSE, F. and SCHEFFER, M. 2009. The angiosperm radiation revisited, an ecological explanation for Darwin's 'abominable mystery'. *Ecology Letters*, **12**, 865–872.

BLAIS, R. A. 1957. Occurrence of upper Cretaceous (?) tree leaves Redmond Mine, province of Labrador, Canada. .

———. 1959. L'origine des minerais crétacés du gisement de fer de Redmond, Labrador. *Le Naturaliste Canadien*, **86**, 265–299.

——— and MCMAHON, D. J. 1958. The Cretaceous flora associated with the iron deposits of the Knob Lake district, Canada. .

BOND, W. J. and SCOTT, A. C. 2010. Fire and the spread of flowering plants in the Cretaceous. *NPH New Phytologist*, **188**, 1137–1150.

BOYD, A. 1993. Paleodepositional setting of the Late Cretaceous Pautût Flora from West Greenland as determined by sedimentological and plant taphonomical data. *Palaeogeography, Palaeoclimatology, Palaeoecology*, **103**, 251–280.

TER BRAAK, C. J. F. 1986. Canonical Correspondence Analysis: A New Eigenvector Technique for Multivariate Direct Gradient Analysis. *Ecology*, **67**, 1167–1179.

BROCK, P. D. 2004. Phasmida (Stick and Leaf Insects). *In* HUTCHINS, M., GARRISON, R. W., GEIST, V., LOISELLE, P. V., SCHLAGER, N., MCDADE, M. C., OLENDORF, D., EVANS, A. V., JACKSON, J. A., KLEIMAN, D. G., MURPHY, J. B., THONEY, D. A., BOCK, W. J., CRAIG, S. F. and DUELLMAN, W. E. (eds.) *Grzimek's Animal Life Encyclopedia*, Vol. 3. Gale, Detroit, 9 pp.

BURNHAM, R. J., PITMAN, N. C. A., JOHNSON, K. R. and WILF, P. 2001. Habitat-related error in estimating temperatures from leaf margins in a humid tropical forest. *American Journal of Botany*, **88**, 1096–1102.

BUTLER, R. J., BARRETT, P. M., KENRICK, P. and PENN, M. G. 2009. Diversity patterns amongst herbivorous dinosaurs and plants during the Cretaceous: implications for hypotheses of dinosaur/angiosperm co-evolution. *JEB Journal of Evolutionary Biology*, **22**, 446–459.

CARLQUIST, S. 1977. Ecological Factors in Wood Evolution: A Floristic Approach. *American Journal of Botany*, **64**, 887–896.

CARPENTER, F. M. 1967. Cretaceous Insects From Labrador 2. A New Family of Snake-Flies (Neuroptera: Alloraphidiidae). *Psyche: A Journal of Entomology*, **74**, 270–275.

COHEN, K. M., HARPER, D. A. T. and GIBBARD, P. L. 2018. *ICS International Chronostratigraphic Chart 2018/08*. International Commission on Stratigraphy, IUGS. Downloaded from www.stratigraphy.org on 15 December 2018.

COIFFARD, C., GOMEZ, B., DAVIERO-GOMEZ, V. and DILCHER, D. L. 2012. Rise to dominance of angiosperm pioneers in European Cretaceous environments. *Proceedings of the National Academy of Sciences*, **109**, 20955–20959.

CONLIFFE, J. 2016. *Geology and Geochemistry of High-Grade Iron-Ore Deposits in the Kivicic, Timmins and Ruth Lake Areas, Western Labrador*. *Current Research*. Newfoundland and Labrador Department of Natural Resources Geological Survey, 26 pp.

———, KERR, A. and HANCHAR, D. 2012. *Iron Ore*. *Mineral Commodities Series*. Newfoundland and Labrador Department of Natural Resources Geological Survey, 15 pp.

CRAGGS, H. J., VALDES, P. J. and WIDDOWSON, M. 2012. Climate model predictions for the latest Cretaceous: An evaluation using climatically sensitive sediments as proxy indicators. *Palaeogeography, Palaeoclimatology, Palaeoecology*, **315–316**, 12–23.

CRANE, P. R., FRIIS, E. M. and PEDERSEN, K. R. 1995. The origin and early diversification of angiosperms. *Nature*, **374**, 27–33.

CRIFÒ, C., CURRANO, E. D., BARESCH, A. and JARAMILLO, C. 2014. Variations in angiosperm leaf vein density have implications for interpreting life form in the fossil record. *Geology*, **42**, 919–922.

DEMERS-POTVIN, A. V. and LARSSON, H. C. E. 2019. *Data from: Palaeoclimatic reconstruction for a Cenomanian-aged angiosperm flora near Schefferville, Labrador*. Dryad Digital Repository. Downloaded from https://datadryad.org/review?doi=doi:10.5061/dryad.bg7pd54 .

DOLPH, G. E. and DILCHER, D. L. 1979. Foliar Physiognomy as an Aid in Determining Paleoclimate. *Palaeontographica Abteilung B*, **170**, 151–172.

DORF, E. 1959. Cretaceous flora from beds associated with rubble iron-ore deposits in the Labrador Trough. *Bulletin of the Geological Society of America*, **70**, 1591.

———. 1967. Cretaceous Insects From Labrador I. Geologic Occurrence. *Psyche: A Journal of Entomology*, **74**, 267–269.

DOYLE, J. A. and HICKEY, L. J. 1977. Pollen and Leaves from the Mid-Cretaceous Potomac Group and Their Bearing on Early Angiosperm Evolution. *In Origin and Early Evolution of Angiosperms*, Columbia University Press, New York, 67 pp.

ELLIS, B., DALY, D. C., HICKEY, L. J., JOHNSON, K. R., MITCHELL, J. D., WILF, P. and WING, S. L. 2009. *Manual of Leaf Architecture*. Cornell University Press,

Ithaca.
EMERSON, A. E. 1967. Cretaceous Insects From Labrador 3. a New Genus and Species of Termite. (Isoptera: Hodotermitidae). *Psyche: A Journal of Entomology*, **74**, 276–289.
FEILD, T. S., BRODRIBB, T. J., IGLESIAS, A., CHATELET, D. S., BARESCH, A., UPCHURCH, G. R., GOMEZ, B., MOHR, B. A. R., COIFFARD, C., KVACEK, J. and JARAMILLO, C. 2011. Fossil evidence for Cretaceous escalation in angiosperm leaf vein evolution. *Proceedings of the National Academy of Sciences of the United States of America*, **108**, 8363–8366.
FLETCHER, T. L., GREENWOOD, D. R., MOSS, P. T. and SALISBURY, S. W. 2014. Paleoclimate of the Late Cretaceous (Cenomanian–Turonian) Portion of the Winton Formation, Central-Western Queensland, Australia: New Observations Based on CLAMP and Bioclimatic Analysis. *PALAIOS*, **29**, 121–128.
GREENWOOD, D. R. 1992. Taphonomic constraints on foliar physiognomie interpretations of Late Cretaceous and tertiary palaeoeclimates. *Review of Palaeobotany and Palynology*, **71**, 149–190.
GREENWOOD, D. R. 2007. Fossil angiosperm leaves and climate: from Wolfe and Dilcher to Burnham and Wilf. *Courier Forschungsinstitut Senckenberg*, **258**, 95–108.
GREENWOOD, D. R., WILF, P., WING, S. L. and CHRISTOPHEL, D. C. 2004. Paleotemperature Estimation Using Leaf-Margin Analysis: Is Australia Different? *PALAIOS*, **19**, 129–142.
GRIMALDI, D. A. 1999. The Co-Radiations of Pollinating Insects and Angiosperms in the Cretaceous. *Annals of the Missouri Botanical Garden*, **86**, 373–406.
——— and ENGEL, M. S. 2005. *Evolution of the insects*. Cambridge University Press, New York.
HARRIS, E. B. and ARENS, N. C. 2016. A mid-Cretaceous angiosperm-dominated macroflora from the Cedar Mountain Formation of Utah, USA. *Journal of Paleontology*, **90**, 640–662.
HERMAN, A. B., SPICER, R. A. and SPICER, T. E. V. 2016. Environmental constraints on terrestrial vertebrate behaviour and reproduction in the high Arctic of the Late Cretaceous. *Palaeogeography, Palaeoclimatology, Palaeoecology*, **441**, 317–338.
HICKEY, L. J. 1973. Classification of the Architecture of Dicotyledonous Leaves. *American Journal of Botany American Journal of Botany*, **60**, 17–33.
——— and DOYLE, J. A. 1977. Early Cretaceous Fossil Evidence for Angiosperm Evolution. *Botanical Review*, **43**, 3–104.
——— and ARMSTRONG, T. B. 1998. A mid-Cretaceous (Cenomanian) Flora from the Interior of the Canadian Shield in Western Labrador. *American Institute of Biological Sciences*, **49 (26.8)**.
VAN HINSBERGEN, D. J. J., DE GROOT, L. V., VAN SCHAIK, S. J., SPAKMAN, W., BIJL, P. K., SLUIJS, A., LANGEREIS, C. G. and BRINKHUIS, H. 2015*a*. *Paleolatitude.org: A Paleolatitude Calculator for Paleoclimate Studies model version 2.1*. Paleolatitude.org. Downloaded from http://www.paleolatitude.org/ on 13 February 2019.
———, ———, ———, ———, BIJL, P. K., SLUIJS, A., LANGEREIS, C. G. and BRINKHUIS, H. 2015*b*. A Paleolatitude Calculator for Paleoclimate Studies.

PLOS ONE, **10**, e0126946.

JACQUES, F. M. B., SHI, G., SU, T. and ZHOU, Z. 2015. A tropical forest of the middle Miocene of Fujian (SE China) reveals Sino-Indian biogeographic affinities. *Review of Palaeobotany and Palynology*, **216**, 76–91.

JONSSON, C. H. W. and HEBDA, R. J. 2015. Macroflora, paleogeography, and paleoecology of the Upper Cretaceous (Turonian?–Santonian) Saanich Member of the Comox Formation, Saanich Peninsula, British Columbia, Canada. *Canadian Journal of Earth Sciences*, **52**, 519–536.

JUD, N. A., D'EMIC, M. D., WILLIAMS, S. A., MATHEWS, J. C., TREMAINE, K. M. and BHATTACHARYA, J. 2018. A new fossil assemblage shows that large angiosperm trees grew in North America by the Turonian (Late Cretaceous). *Science Advances*, **4**, eaar8568.

KOTTEK, M., GRIESER, J., BECK, C., RUDOLF, B. and RUBEL, F. 2006. World Map of the Köppen-Geiger climate classification updated. *Meteorologische Zeitschrift*, **15**, 259–263.

KOWALSKI, E. A. and DILCHER, D. L. 2003. Warmer paleotemperatures for terrestrial ecosystems. *Proceedings of the National Academy of Sciences*, **100**, 167–170.

LESQUEREUX, L. 1892. The Flora of the Dakota Group: A Posthumous Work. *Monographs of the U. S. Geological Survey*, **17**.

LI, Y., WANG, Z., XU, X., HAN, W., WANG, Q., ZOU, D. and JORDAN, G. 2016. Leaf margin analysis of Chinese woody plants and the constraints on its application to palaeoclimatic reconstruction. *GEB Global Ecology and Biogeography*, **25**, 1401–1415.

LITTLE, S. A., KEMBEL, S. W. and WILF, P. 2010. Paleotemperature Proxies from Leaf Fossils Reinterpreted in Light of Evolutionary History. *PLOS ONE*, **5**, e15161.

LUPIA, R., CRANE, P. R. and LIDGARD, S. 2000. Angiosperm diversification and Cretaceous environmental change. *In* CULVER, S. J. and RAWSON, P. F. (eds.) *Biotic Response to Global Change*, Cambridge University Press, Cambridge, 15 pp.

MACNEAL, D. 1958. *Flora of the Upper Cretaceous Woodbine Sand in Denton County, Texas*. Academy of Natural Sciences.

MILLER, I. M., BRANDON, M. T. and HICKEY, L. J. 2006. Using leaf margin analysis to estimate the mid-Cretaceous (Albian) paleolatitude of the Baja BC block. *Earth and Planetary Science Letters*, **245**, 95–114.

NEW, M., HULME, M. and JONES, P. 1999. Representing Twentieth-Century Space–Time Climate Variability. Part I: Development of a 1961–90 Mean Monthly Terrestrial Climatology. *Journal of Climate*, **12**, 829–856.

NEWBERRY, J. S. 1886. The Flora of the Amboy Clays. *Bulletin of the Torrey Botanical Club*, **13**, 33–37.

OGG, J. G., AGTERBERG, F. P. and GRADSTEIN, F. M. 2004. The Cretaceous Period. *In* GRADSTEIN, F. M., OGG, J. G. and SMITH, A. G. (eds.) *A Geologic Time Scale 2004*, Cambridge University Press, Cambridge, UK; New York, 39 pp.

PARRISH, J. T. and SPICER, R. A. 1988. Late Cretaceous terrestrial vegetation: A near-polar temperature curve. *Geology*, **16**, 22–25.

PEPPE, D. J., ROYER, D. L., CARIGLINO, B., OLIVER, S. Y., NEWMAN, S.,

LEIGHT, E., ENIKOLOPOV, G., FERNANDEZ-BURGOS, M., HERRERA, F., ADAMS, J. M., CORREA, E., CURRANO, E. D., ERICKSON, J. M., HINOJOSA, L. F., HOGANSON, J. W., IGLESIAS, A., JARAMILLO, C. A., JOHNSON, K. R., JORDAN, G. J., KRAFT, N. J. B., LOVELOCK, E. C., LUSK, C. H., NIINEMETS, U., PEÒUELAS, J., RAPSON, G., WING, S. L. and WRIGHT, I. J. 2011. Sensitivity of leaf size and shape to climate: global patterns and paleoclimatic applications. *New Phytologist*, **190**, 724–739.

PHILIPPE, M., GOMEZ, B., GIRARD, V., COIFFARD, C., DAVIERO-GOMEZ, V., THEVENARD, F., BILLON-BRUYAT, J.-P., GUIOMAR, M., LATIL, J.-L., LE LOEUFF, J., NÉRAUDEAU, D., OLIVERO, D. and SCHLÖGL, J. 2008. Woody or not woody? Evidence for early angiosperm habit from the Early Cretaceous fossil wood record of Europe. *Palaeoworld*, **17**, 142–152.

PICARD, M. D. and HIGH, L. R. 1972. Criteria for Recognizing Lacustrine Rocks. *Society of Economic Paleontologists and Mineralogists Special Publication*, **16**, 108–145.

PONOMARENKO, A. G. 1969. Cretaceous Insects From Labrador. 4. A New Family of Beetles (Coleoptera: Archostemata). *Psyche: A Journal of Entomology*, **76**, 306–310.

RETALLACK, G. J. and DILCHER, D. L. 1986. Cretaceous angiosperm invasion of North America. *Cretaceous Research*, **7**, 227–252.

RICE, H. M. A. 1969. An Antlion (Neuroptera) and a Stonefly (Plecoptera) of Cretaceous Age from Labrador, Newfoundland. *Geological Survey of Canada, Department of Energy, Mines and Resources, Paper*, **68–65**, iv + 1-11.

ROYER, D. L., MILLER, I. M., PEPPE, D. J. and HICKEY, L. J. 2010. Leaf economic traits from fossils support a weedy habit for early angiosperms. *American Journal of Botany*, **97**, 438–445.

———, WILF, P., JANESKO, D. A., KOWALSKI, E. A. and DILCHER, D. L. 2005. Correlations of climate and plant ecology to leaf size and shape: Potential proxies for the fossil record. *American Journal of Botany*, **92**, 1141–1151.

SCHINDELIN, J., ARGANDA-CARRERAS, I., FRISE, E., KAYNIG, V., LONGAIR, M., PIETZSCH, T., PREIBISCH, S., RUEDEN, C., SAALFELD, S., SCHMID, B., TINEVEZ, J.-Y., WHITE, D. J., HARTENSTEIN, V., ELICEIRI, K., TOMANCAK, P. and CARDONA, A. 2012. Fiji: an open-source platform for biological-image analysis. *Nature Methods*, **9**, 676–682.

SÉGUIN, M. K. 1971. Discovery of Direct-Shipping Iron Ore by Geophysical Methods in the Central Part of the Labrador Trough. *Geophysical Prospecting*, **19**, 459–486.

SPICER, R. A. 2006. *CLAMP*. Downloaded from http://clamp.ibcas.ac.cn/CLAMP_Home.html on 13 April 2018.

——— and PARRISH, J. T. 1986. Paleobotanical evidence for cool north polar climates in middle Cretaceous (Albian-Cenomanian) time. *Geology*, **14**, 703–706.

——— and HERMAN, A. B. 2001. The Albian-Cenomanian flora of the Kukpowruk River, western North Slope, Alaska: stratigraphy, palaeofloristics, and plant communities. *Cretaceous Research*, **22**, 1–40.

——— and ———. 2010. The Late Cretaceous environment of the Arctic: A quantitative reassessment based on plant fossils. *Palaeogeography,*

Palaeoclimatology, Palaeoecology, **295**, 423–442.

SPICER, R. A., AHLBERG, A., HERMAN, A. B., KELLEY, S. P., RAIKEVICH, M. I. and REES, P. M. 2002. Palaeoenvironment and ecology of the middle Cretaceous Grebenka flora of northeastern Asia. *Palaeogeography, Palaeoclimatology, Palaeoecology*, **184**, 65–105.

SPICER, R. A., AHLBERG, A., HERMAN, A. B., HOFMANN, C.-C., RAIKEVICH, M., VALDES, P. J. and MARKWICK, P. J. 2008. The Late Cretaceous continental interior of Siberia: A challenge for climate models. *Earth and Planetary Science Letters*, **267**, 228–235.

SPICER, R. A., VALDES, P. J., SPICER, T. E. V., CRAGGS, H. J., SRIVASTAVA, G., MEHROTRA, R. C. and YANG, J. 2009. New developments in CLAMP: Calibration using global gridded meteorological data. *Palaeogeography, Palaeoclimatology, Palaeoecology*, **283**, 91–98.

TORSVIK, T. H., VAN DER VOO, R., PREEDEN, U., MAC NIOCAILL, C., STEINBERGER, B., DOUBROVINE, P. V., VAN HINSBERGEN, D. J. J., DOMEIER, M., GAINA, C., TOHVER, E., MEERT, J. G., MCCAUSLAND, P. J. A. and COCKS, L. R. M. 2012. Phanerozoic polar wander, palaeogeography and dynamics. *Earth-Science Reviews*, **114**, 325–368.

TREMBLAY, A., RODEN-TICE, M. K., BRANDT, J. A. and MEGAN, T. W. 2013. Mesozoic fault reactivation along the St. Lawrence rift system, eastern Canada: Thermochronologic evidence from apatite fission-track dating. *GSA Bulletin*, **125**, 794–810.

UPCHURCH, G. R. and DILCHER, D. L. 1990. Cenomanian angiosperm leaf megafossils, Dakota Formation, Rose Creek locality, Jefferson County, southeastern Nebraska. *U.S. Geological Survey bulletin, v.1915*, 1–55.

USHER, J. 1954. Brown « Coal » in the Labrador Trough; Abstract. *Bulletin of the Geological Society of America*, **6**, 99–101.

WHITE, T. S., WITZKE, B. J. and LUDVIGSON, G. A. 2000. Evidence for an Albian Hudson arm connection between the Cretaceous Western Interior Seaway of North America and the Labrador Sea. *Geological Society of America Bulletin*, **112**, 1342–1355.

WILF, P. 1997. When are leaves good thermometers? A new case for Leaf Margin Analysis. *Paleobiology*, **23**, 373–390.

WING, S. L. and GREENWOOD, D. R. 1993. Fossils and fossil climate: the case for equable continental interiors in the Eocene. *Phil. Trans. R. Soc. Lond. B*, **341**, 243–252.

WOLFE, J. A. 1979. Temperature parameters of humid to mesic forests of Eastern Asia and relation to forests of other regions of the Northern Hemisphere and Australasia: analysis of temperature data from more than 400 stations in Eastern Asia. *U.S. Geological Survey Professional Paper*, **1106**, 1–37.

———. 1993. A Method of Obtaining Climatic Parameters from Leaf Assemblages. *In US Geological Survey Bulletin 2040*, U.S. Government Printing Office, 73 pp.

——— and UPCHURCH, G. R. 1987. North American nonmarine climates and vegetation during the Late Cretaceous. *Palaeogeography, Palaeoclimatology, Palaeoecology*, **61**, 33–77.

YANG, J., SPICER, R. A., SPICER, T. E. V. and LI, C.-S. 2011. 'CLAMP Online': a

new web-based palaeoclimate tool and its application to the terrestrial Paleogene and Neogene of North America. *Palaeobiodiversity and Palaeoenvironments*, **91**, 163.

———, ———, ———, ARENS, N. C., JACQUES, F. M. B., SU, T., KENNEDY, E. M., HERMAN, A. B., STEART, D. C., SRIVASTAVA, G., MEHROTRA, R. C., VALDES, P. J., MEHROTRA, N. C., ZHOU, Z.-K. and LAI, J.-S. 2015. Leaf form–climate relationships on the global stage: an ensemble of characters. *Global Ecology and Biogeography*, **24**, 1113–1125.

ZAJAC, I. S. 1974. The stratigraphy and mineralogy of the Sokoman Formation in the Knob Lake area, Quebec and Newfoundland. *Geological Survey of Canada Bulletin*, **220**, 1–159.

FIG. 1. Situation of the Redmond Formation in geologic time and in space. (**A**) Geological timescale placing the Redmond Formation in the context of major Cretaceous environmental trends. Absolute ages based on the ICS International Chronostratigraphic Chart (Cohen *et al.* 2018). Timing of oceanic anoxic events from Ogg *et al*. (2004). Relative diversity of major plant groups based on Butler et al. (2009). (**B**) Location of the Redmond Formation near Schefferville in Labrador (54°41'N, 66°45'W). Exposures of the Sokoman Formation based on Conliffe (2016).

FIG. 2. Some representatives of the non-angiosperm organisms preserved from the Redmond ecosystem. (**A**) Two young curled fern fronds (Gleicheniales), RMPB 2018.18.30. (**B**) Partial leaf of the cupressaceous conifer *Widdringtonites subtilis* Heer, YPM 30546. (**C**) Partial leaf of the pinaceous conifer *Abietites longifolius* (Fontaine) Berry, RMPB 2018.18.29. (**D**) Isolated fern frond attributed to *Asplenium angustipinnata* Fontaine (Polypodiales), YPM 30541. (**E**) Partial leaf of the cupressaceous conifer *Sequoia gracillima* (Lesquereux) Newberry, YPM 30529. Plants identified by Hickey (notes left alongside specimens). Scale bars 1 cm. Images adjusted for brightness and contrast.

FIG. 3. Some invertebrate remains indicative of the Redmond Formation's palaeoclimate and depositional environment. (**A**) Almost complete undescribed mayfly nymph (Ephemeroptera; Hexagenitidae), MPEP 1156.5. (**B**) Folded wings of large phasmatodean *Palaeopteron complexum* Rice 1969, GSC 22189. (**C**) Articulated scutellum and elytra of undescribed water beetle (Coleoptera; Adephaga; Hydradephaga), MPEP 702.4. (**D**) Isolated fore wing of termite (Hodotermitidae) *Cretatermes carpenteri* Emerson 1967, YPM 223802. (**E**) Isolated fore wing of snakefly (Alloraphidiidae) *Alloraphidia dorfi* Carpenter 1967, YPM 223803. (**F**) Ichnofossil of unknown burrowing benthic invertebrate, MPEP 702.41. **A**, **C** and **F** represent autochthonous remains from a lacustrine depositional environment; **B**, **D** and **E** represent allochthonous remains indicative of a warm palaeoclimate. Scale bars 5mm unless specified otherwise. Images adjusted for brightness and contrast.

FIG. 4. Representative specimens of the angiosperm morphotypes from the Redmond Formation. Morphotype 1 ('*Andromeda' novaecaesarae* Hollick): (**A**) YPM 47190. Morphotype 2 ('*Andromeda' parlatorii* Heer): (**B**) YPM 30413. Morphotype 3 ('*Aralia*' *groenlandica* Heer): (**C**) YPM 30445, (**D**) YPM 30384. Morphotype 4 (*Araliopsoides cretacea* (Newberry) Berry): (**E**) YPM 47191. Morphotype 5 (*Celastrophyllum albaedomus* Ward): (**F**) YPM 47192. Morphotype 7 (*Cissites formosus* Heer): (**H**) YPM 47247. Morphotype 8 (*Cissites platanoidea* Hollick): (**G**) MPEP 702.53, (**I**) YPM 30423, (**J**) YPM 30428, (**K**) YPM 47248. Morphotype 6 (*Celastrophyllum brittonianum* Hollick): (**L**) YPM 47246. Morphotype 10 (*Daphnophyllum dakotense* Lesquereux): (**M**) YPM 30492. Morphotype 9 (*Crassidenticulum* n. sp. Indet): (**N**) YPM 30471. Scale bars 1 cm. Images adjusted for brightness and contrast. For more information on each morphotype, see Demers-Potvin and Larsson (2019).

FIG. 5. Representative specimens of the angiosperm morphotypes from the Redmond Formation. Morphotype 11 (‘*Densinervum*’ *kaulii* Upchurch & Dilcher): (**A**) YPM 30448. Morphotype 12 (*Dicotylophyllum* n. sp. Indet): (**B**) YPM 30465. Morphotype 13 (‘*Diospyros’ primaeva* Heer): (**C**) YPM 47249. Morphotype 14 (*Dryandroides lancelota* Knowlton): (**D**) YPM 47294. Morphotype 15 (*Dryandroides* n. sp. Indet): (**E**) MPEP 609.6. Morphotype 16 (*Ficus berthoudi* Lesquereux): (**F**) YPM 47296. Morphotype 18 (*Liriodendropsis simplex* (Newberry) Newberry): (**G**) YPM 45137. Morphotype 19 (*Magnolia amplifolia* Heer, *Magnolia speciosa* Heer): (**H**) YPM 30401. Morphotype 17 (*Liriodendron simplex* Newberry): (**I**) YPM 30484. Morphotype 20 (*Magnolia* n. sp. Indet): (**J**) YPM 30405. Scale bars 1 cm. Images adjusted for brightness and contrast. For more information on each morphotype, see Demers-Potvin and Larsson (2019).

FIG. 6. Representative specimens of the angiosperm morphotypes from the Redmond Formation. Morphotype 21 (*Menispermites obtusiloba* Lesquereux): (**A**) YPM 30521. Morphotype 22 (*Menispermites trilobatus* Berry): (**B**) YPM 30516. Morphotype 23 ('*Platanus*' *heerii* Lesquereux): (**C**) YPM 30517. Morphotype 26 (*Sassafras acutilobum* Lesquereux) : (**D**) YPM 30375, (**E**) YPM 30390, (**F**) RMPB 2018.18.27. Morphotype 25 (*Salix newberryana* Hollick): (**G**) YPM 47303. Morphotype 28: (**H**) RMPB 2018.18.9. Morphotype 24 ('*Platanus*' *shirleyensis* Berry): (**I**) YPM 30392. Morphotype 27 ('*Sterculia*' *lugubris* Lesquereux): (**J**) YPM 47299. Morphotype 31: (**K**) RMPB 2018.18.13. Morphotype 29: (**L**) YPM 47300. Morphotype 30: (**M**) YPM 47301. Morphotype 33: (**N**) MPEP 702.59. Morphotype 46: (**O**) MPEP 1177.9. Scale bars 1 cm. Images adjusted for brightness and contrast. For more information on each morphotype, see Demers-Potvin and Larsson (2019).

936 FIG. 7. Representative specimens of the angiosperm morphotypes from the Redmond Formation. Morphotype 32: (**A**) YPM 30500. Morphotype 38: (**B**) GSC 104192.
938 Morphotype 35: (**C**) MPEP 702.58. Morphotype 36: (**D**) MPEP 609.1. Morphotype 34: (**E**) MPEP 702.39. Morphotype 37: (**F**) MPEP 702.115. Morphotype 41: (**G**) RMPB
940 2018.18.2. Morphotype 39: (**H**) RMPB 2018.18.28. Morphotype 45: (**I**) MPEP 1152.27. Morphotype 42: (**J**) RMPB 2018.18.20. Morphotype 40: (**K**) RMPB 2018.18.4.
942 Morphotype 43: (**L**) MPEP 1151.5. Morphotype 44: (**M**) MPEP 1154.5. Scale bars 1 cm. Images adjusted for brightness and contrast. For more information on each morphotype,
944 see Demers-Potvin and Larsson (2019).

FIG. 8. Implied palaeolatitudinal gradients of mean annual temperature for a Cenomanian age bin (93.9 - 100.5 MA) based on two palaeoclimate estimate methods: CLAMP (this study) and LMA (reproduced from Miller *et al*. (2006)). Palaeolatitudes calculated from van Hinsbergen *et al*. (2015*a*). In the following list, each flora is succeeded by its estimated palaeolatitude and the source of its palaeoclimate estimate. Raritan (36.4°N) (Wolfe and Upchurch 1987); Patapsco (36.4°N) (Wolfe and Upchurch 1987); Tuscaloosa (31.7°N) (Spicer and Herman 2010); Woodbine (37.4°N) (Wolfe and Upchurch 1987 (LMA); Spicer and Herman 2010 (CLAMP)); Rose Creek (40.2°N) (this study); Fort Harker (Dakota) (39.0°N) (Wolfe & Upchurch, 1987 (LMA); this study (CLAMP)); Redmond (Redmond) (48.8°N) (Hickey and Armstrong 1998 (LMA); this study (CLAMP)); Dunvegan (58.4°N) (Wolfe and Upchurch 1987); Chandler (78.0°N) (Parrish and Spicer 1988); Nanushuk (79.5°N) (Herman *et al.* 2016). Minimum and maximum palaeolatitude estimates for each point projected as error bars. Abbreviations for the methods used are as follows: Climate Leaf Analysis Multivariate Program (CLAMP), Leaf Margin Analysis (LMA). Regression equations – LMA $y = -0.3228x + 35.415$, $R^2 = 0.8576$. CLAMP $y = -0.1412x + 23.109$, $R^2 = 0.8515$.

TABLE 1. Summary of woody dicotyledonous morphotypes used for a palaeoclimate estimate of the Labrador's Cenomanian Redmond ecosystem.

TABLE 2. Summary of palaeoclimate parameter estimates from the Climate Leaf Analysis Multivariate Program (CLAMP) for the Redmond no.1 site.

TABLE 3. Palaeoclimate estimates for late Albian-Cenomanian North American floras using CLAMP and LMA.

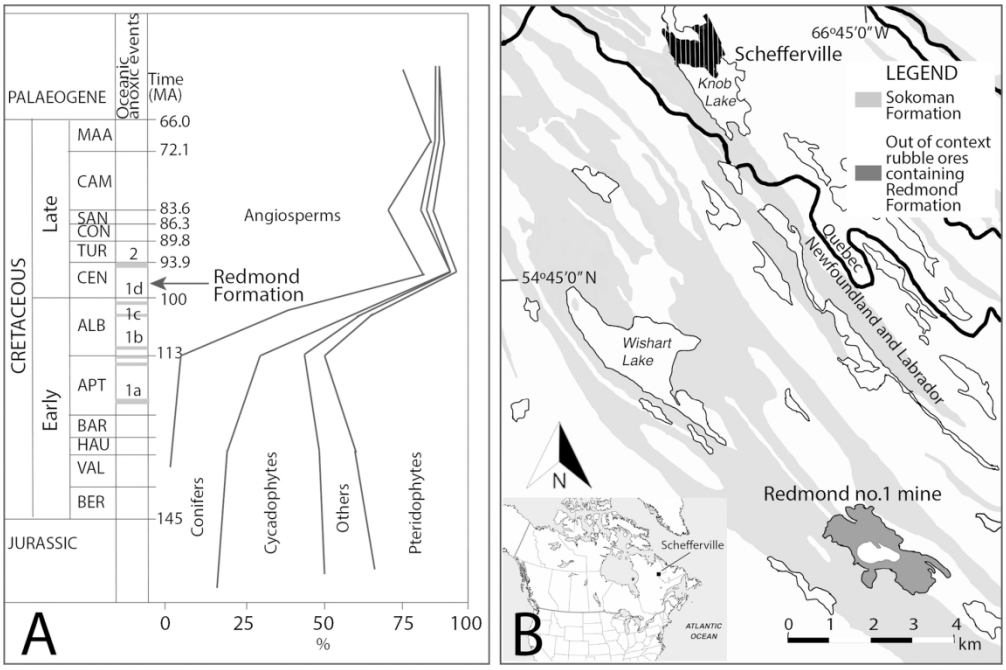

FIG. 1. Situation of the Redmond Formation in geologic time and in space. (A) Geological timescale placing the Redmond Formation in the context of major Cretaceous environmental trends. Absolute ages based on the ICS International Chronostratigraphic Chart (Cohen et al. 2018). Timing of oceanic anoxic events from Ogg et al. (2004). Relative diversity of major plant groups based on Butler et al. (2009). (B) Location of the Redmond Formation near Schefferville in Labrador (54°41′N, 66°45′W). Exposures of the Sokoman Formation based on Conliffe (2016).

165x109mm (300 x 300 DPI)

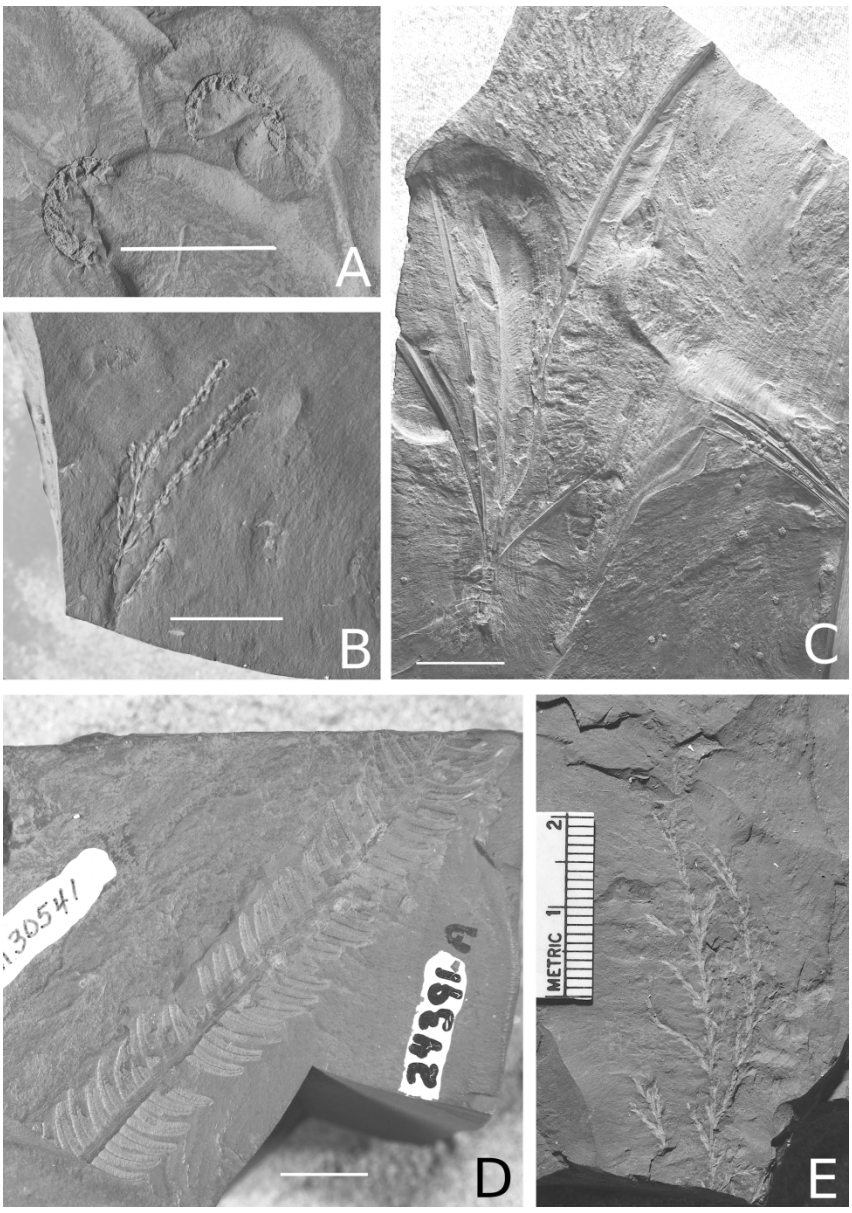

FIG. 2. Some representatives of the non-angiosperm organisms preserved from the Redmond ecosystem. (A) Two young curled fern fronds (Gleicheniales), RMPB 2018.18.30. (B) Partial leaf of the cupressaceous conifer *Widdringtonites subtilis* Heer, YPM 30546. (C) Partial leaf of the pinaceous conifer *Abietites longifolius* (Fontaine) Berry, RMPB 2018.18.29. (D) Isolated fern frond attributed to *Asplenium angustipinnata* Fontaine (Polypodiales), YPM 30541. (E) Partial leaf of the cupressaceous conifer *Sequoia gracillima* (Lesquereux) Newberry, YPM 30529. Plants identified by Hickey (notes left alongside specimens). Scale bars 1 cm. Images adjusted for brightness and contrast.

165x234mm (300 x 300 DPI)

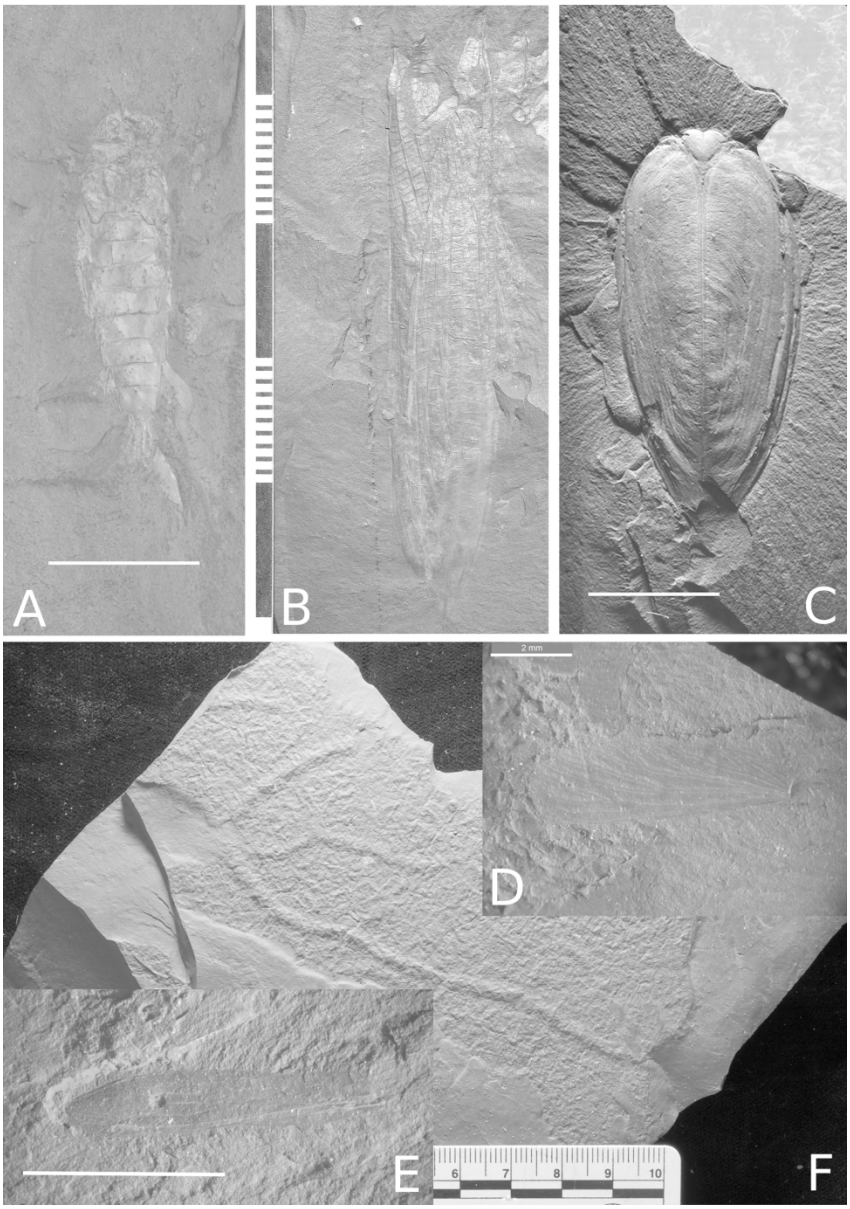

FIG. 3. Some invertebrate remains indicative of the Redmond Formation's palaeoclimate and depositional environment. (A) Almost complete undescribed mayfly nymph (Ephemeroptera; Hexagenitidae), MPEP 1156.5. (B) Folded wings of large phasmatodean *Palaeopteron complexum* Rice 1969, GSC 22189. (C) Articulated scutellum and elytra of undescribed water beetle (Coleoptera; Adephaga; Hydradephaga), MPEP 702.4. (D) Isolated fore wing of termite (Hodotermitidae) *Cretatermes carpenteri* Emerson 1967, YPM 223802. (E) Isolated fore wing of snakefly (Alloraphidiidae) *Alloraphidia dorfi* Carpenter 1967, YPM 223803. (F) Ichnofossil of unknown burrowing benthic invertebrate, MPEP 702.41. A, C and F represent autochthonous remains from a lacustrine depositional environment; B, D and E represent allochthonous remains indicative of a warm palaeoclimate. Scale bars 5 mm unless specified otherwise. Images adjusted for brightness and contrast.

164x233mm (300 x 300 DPI)

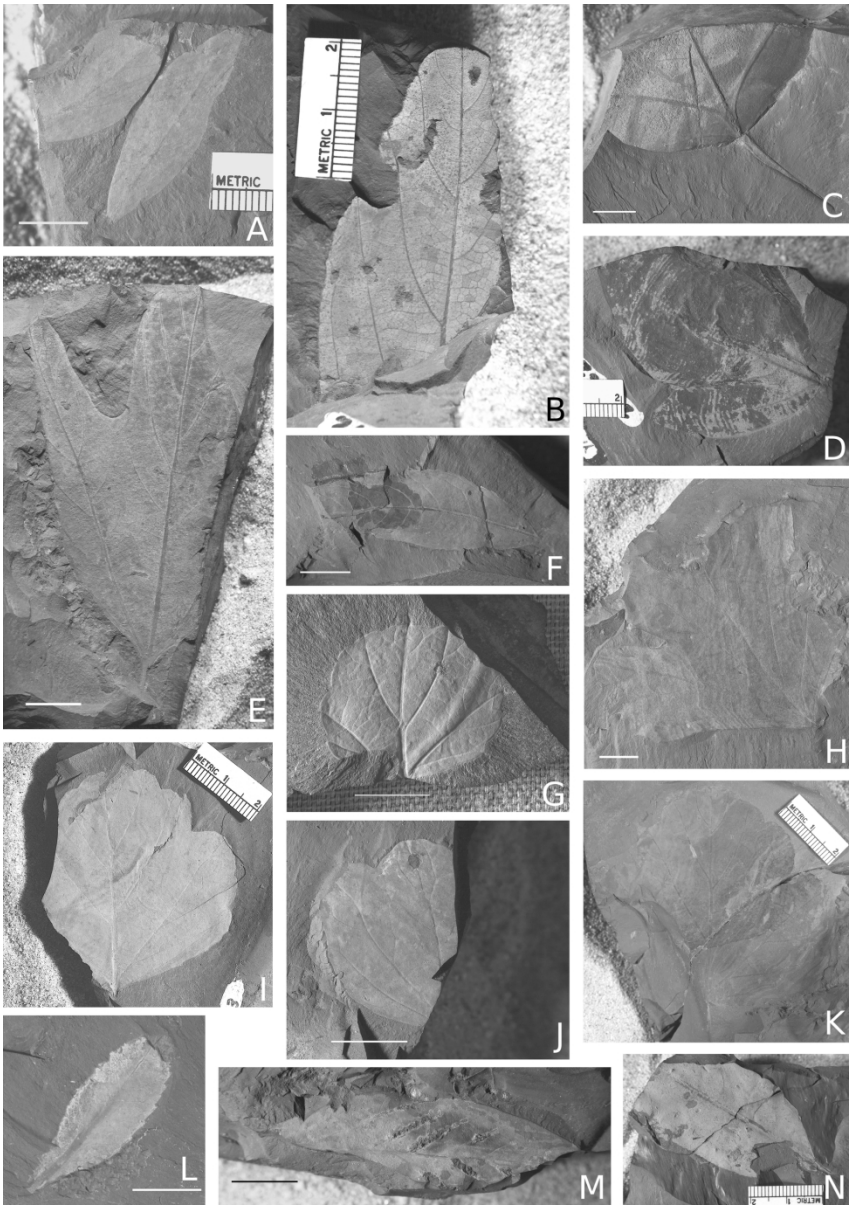

FIG. 4. Representative specimens of the angiosperm morphotypes from the Redmond Formation. Morphotype 1 (*'Andromeda' novaecaesarae* Hollick): (A) YPM 47190. Morphotype 2 (*'Andromeda' parlatorii* Heer): (B) YPM 30413. Morphotype 3 (*'Aralia' groenlandica* Heer): (C) YPM 30445, (D) YPM 30384. Morphotype 4 (*Araliopsoides cretacea* (Newberry) Berry): (E) YPM 47191. Morphotype 5 (*Celastrophyllum albaedomus* Ward): (F) YPM 47192. Morphotype 7 (*Cissites formosus* Heer): (H) YPM 47247. Morphotype 8 (*Cissites platanoidea* Hollick): (G) MPEP 702.53, (I) YPM 30423, (J) YPM 30428, (K) YPM 47248. Morphotype 6 (*Celastrophyllum brittonianum* Hollick): (L) YPM 47246. Morphotype 10 (*Daphnophyllum dakotense* Lesquereux): (M) YPM 30492. Morphotype 9 (*Crassidenticulum* n. sp. Indet): (N) YPM 30471. Scale bars 1 cm. Images adjusted for brightness and contrast. For more information on each morphotype, see Demers-Potvin and Larsson (2019).

165x234mm (300 x 300 DPI)

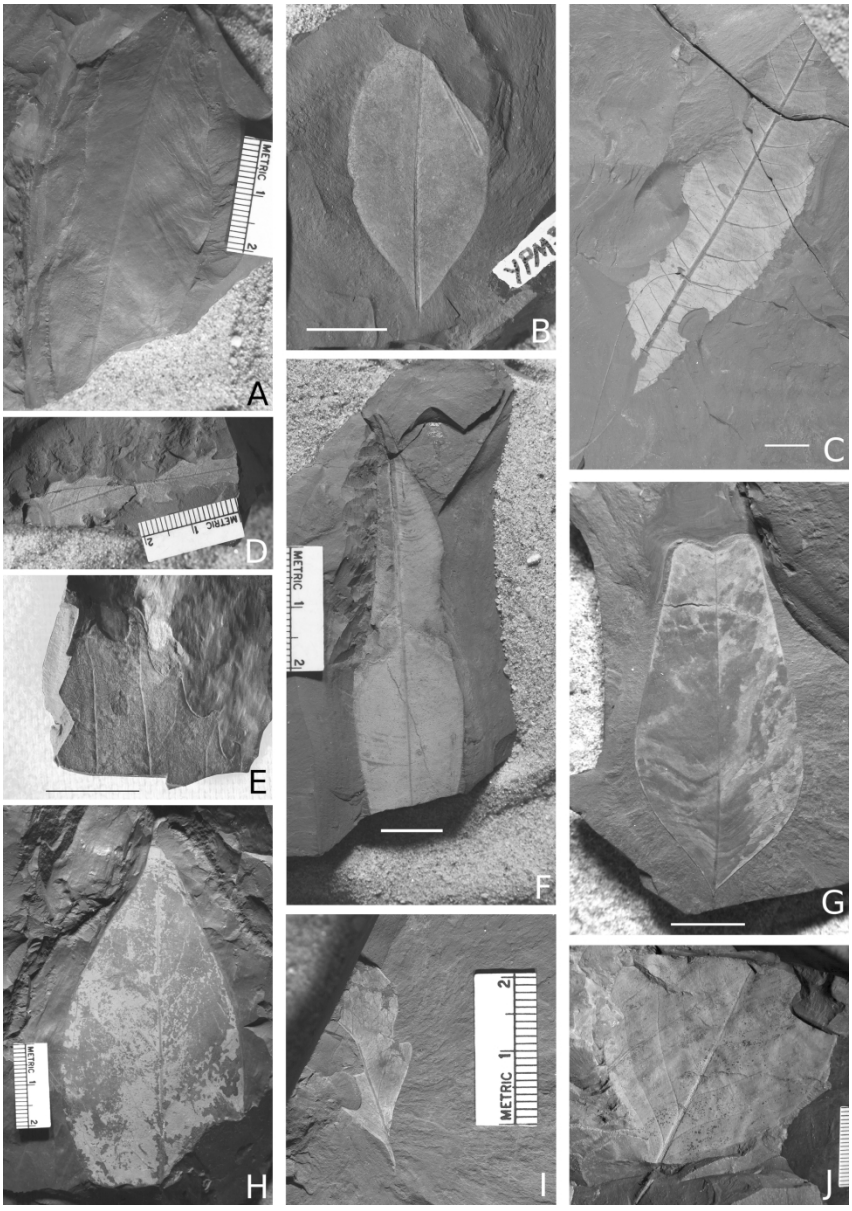

FIG. 5. Representative specimens of the angiosperm morphotypes from the Redmond Formation. Morphotype 11 (*'Densinervum' kaulii* Upchurch & Dilcher): (A) YPM 30448. Morphotype 12 (*Dicotylophyllum* n. sp. Indet): (B) YPM 30465. Morphotype 13 (*'Diospyros' primaeva* Heer): (C) YPM 47249. Morphotype 14 (*Dryandroides lancelota* Knowlton): (D) YPM 47294. Morphotype 15 (*Dryandroides* n. sp. Indet): (E) MPEP 609.6. Morphotype 16 (*Ficus berthoudi* Lesquereux): (F) YPM 47296. Morphotype 18 (*Liriodendropsis simplex* (Newberry) Newberry): (G) YPM 45137. Morphotype 19 (*Magnolia amplifolia* Heer, *Magnolia speciosa* Heer): (H) YPM 30401. Morphotype 17 (*Liriodendron simplex* Newberry): (I) YPM 30484. Morphotype 20 (*Magnolia* n. sp. Indet): (J) YPM 30405. Scale bars 1 cm. Images adjusted for brightness and contrast. For more information on each morphotype, see Demers-Potvin and Larsson (2019).

165x234mm (300 x 300 DPI)

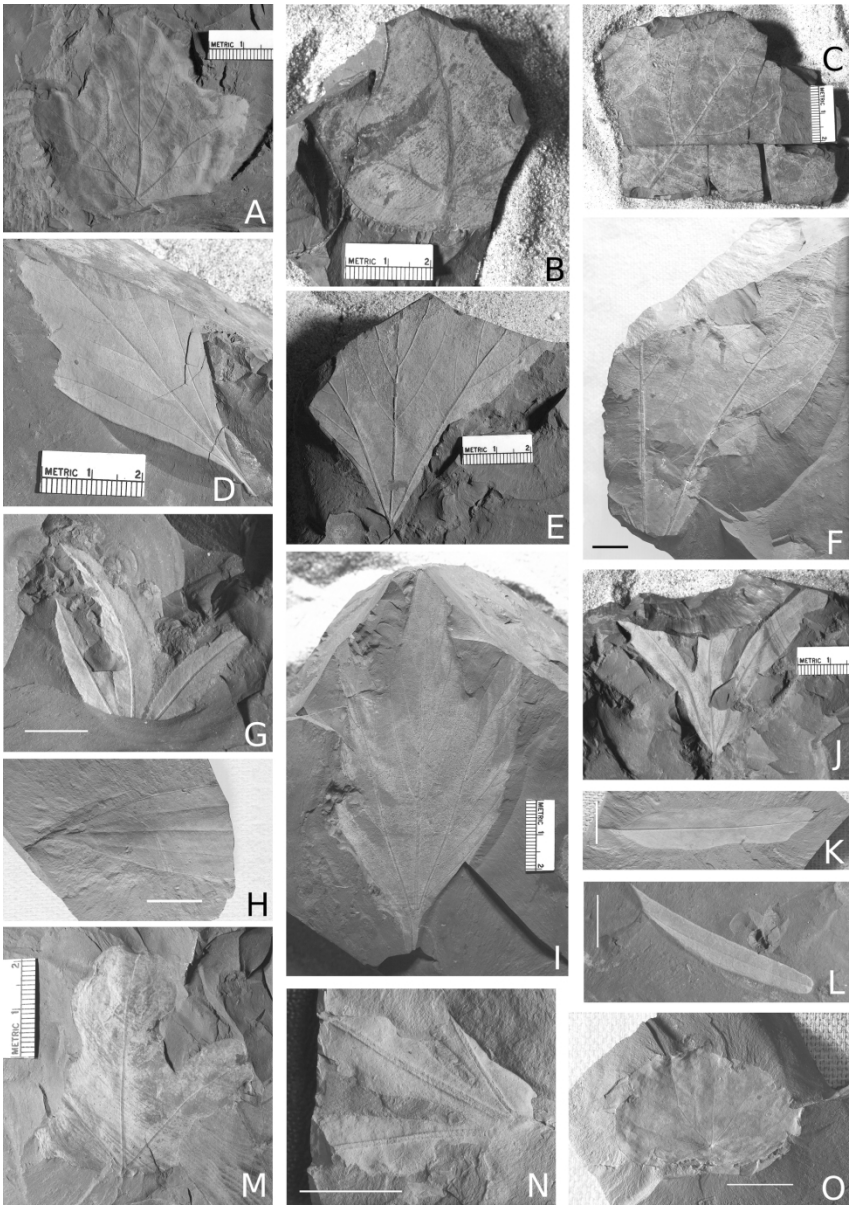

FIG. 6. Representative specimens of the angiosperm morphotypes from the Redmond Formation. Morphotype 21 (*Menispermites obtusiloba* Lesquereux): (A) YPM 30521. Morphotype 22 (*Menispermites trilobatus* Berry): (B) YPM 30516. Morphotype 23 (*'Platanus' heerii* Lesquereux): (C) YPM 30517. Morphotype 26 (*Sassafras acutilobum* Lesquereux) : (D) YPM 30375, (E) YPM 30390, (F) RMPB 2018.18.27. Morphotype 25 (*Salix newberryana* Hollick): (G) YPM 47303. Morphotype 28: (H) RMPB 2018.18.9. Morphotype 24 (*'Platanus' shirleyensis* Berry): (I) YPM 30392. Morphotype 27 (*'Sterculia' lugubris* Lesquereux): (J) YPM 47299. Morphotype 31: (K) RMPB 2018.18.13. Morphotype 29: (L) YPM 47300. Morphotype 30: (M) YPM 47301. Morphotype 33: (N) MPEP 702.59. Morphotype 46: (O) MPEP 1177.9. Scale bars 1 cm. Images adjusted for brightness and contrast. For more information on each morphotype, see Demers-Potvin and Larsson (2019).

165x234mm (300 x 300 DPI)

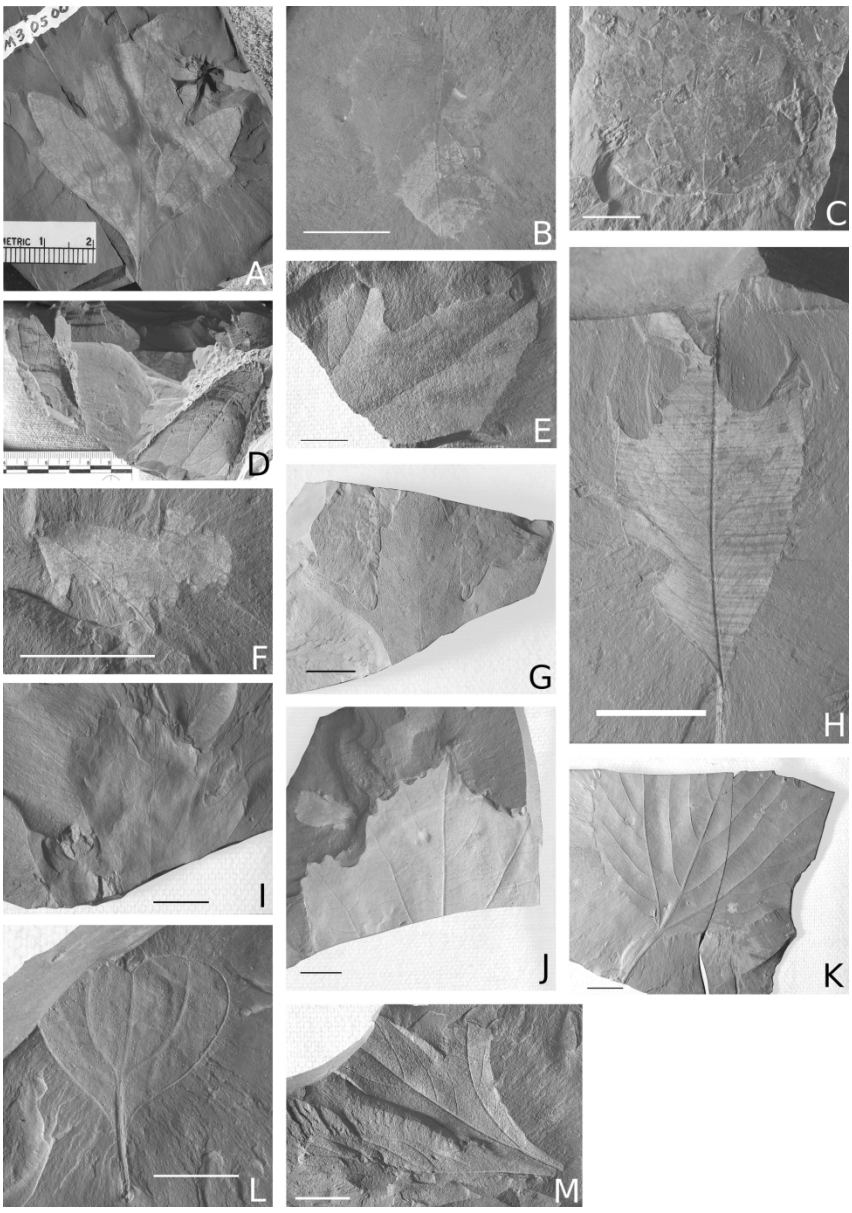

FIG. 7. Representative specimens of the angiosperm morphotypes from the Redmond Formation. Morphotype 32: (A) YPM 30500. Morphotype 38: (B) GSC 104192. Morphotype 35: (C) MPEP 702.58. Morphotype 36: (D) MPEP 609.1. Morphotype 34: (E) MPEP 702.39. Morphotype 37: (F) MPEP 702.115. Morphotype 41: (G) RMPB 2018.18.2. Morphotype 39: (H) RMPB 2018.18.28. Morphotype 45: (I) MPEP 1152.27. Morphotype 42: (J) RMPB 2018.18.20. Morphotype 40: (K) RMPB 2018.18.4. Morphotype 43: (L) MPEP 1151.5. Morphotype 44: (M) MPEP 1154.5. Scale bars 1 cm. Images adjusted for brightness and contrast. For more information on each morphotype, see Demers-Potvin and Larsson (2019).

165x234mm (300 x 300 DPI)

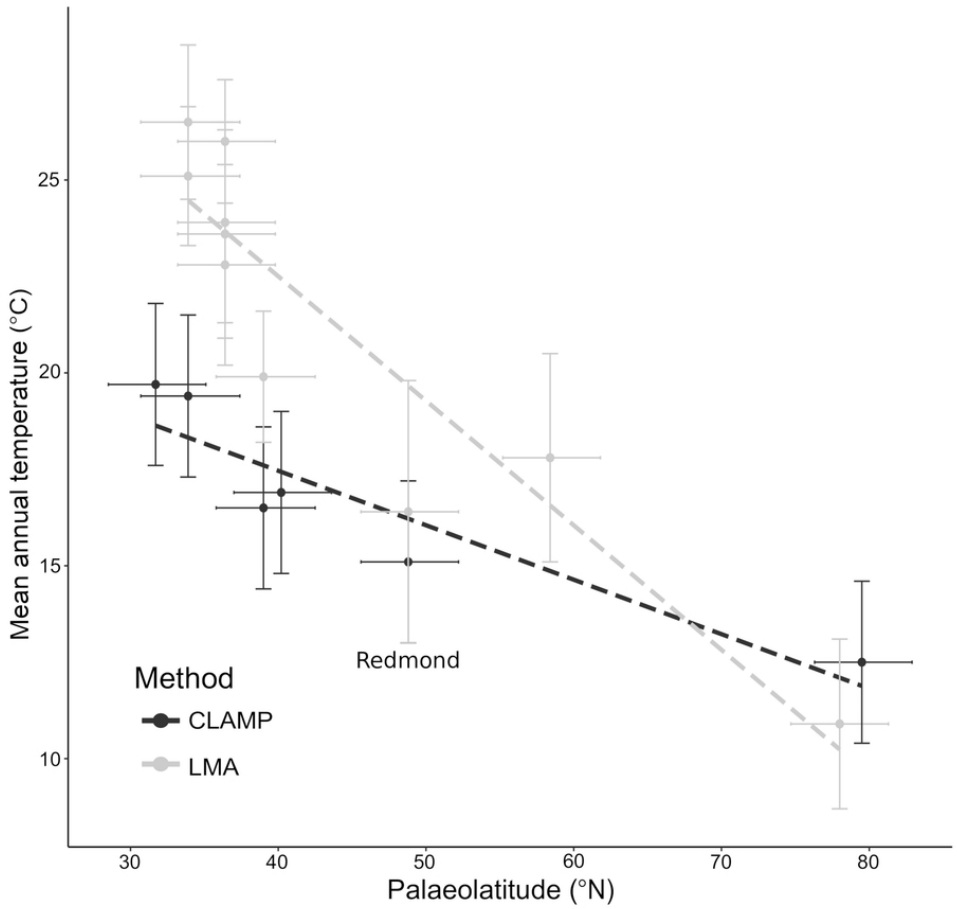

FIG. 8. Implied palaeolatitudinal gradients of mean annual temperature for a Cenomanian age bin (93.9 - 100.5 MA) based on two palaeoclimate estimate methods: CLAMP (this study) and LMA (reproduced from Miller et al. (2006)). Palaeolatitudes calculated from van Hinsbergen et al. (2015a). In the following list, each flora is succeeded by its estimated palaeolatitude and the source of its palaeoclimate estimate. Raritan (36.4°N) (Wolfe and Upchurch 1987); Patapsco (36.4°N) (Wolfe and Upchurch 1987); Tuscaloosa (31.7°N) (Spicer and Herman 2010); Woodbine (37.4°N) (Wolfe and Upchurch 1987 (LMA); Spicer and Herman 2010 (CLAMP)); Rose Creek (40.2°N) (this study); Fort Harker (Dakota) (39.0°N) (Wolfe & Upchurch, 1987 (LMA); this study (CLAMP)); Redmond (Redmond) (48.8°N) (Hickey and Armstrong 1998 (LMA); this study (CLAMP)); Dunvegan (58.4°N) (Wolfe and Upchurch 1987); Chandler (78.0°N) (Parrish and Spicer 1988); Nanushuk (79.5°N) (Herman et al. 2016). Minimum and maximum palaeolatitude estimates for each point projected as error bars. Abbreviations for the methods used are as follows: Climate Leaf Analysis Multivariate Program (CLAMP), Leaf Margin Analysis (LMA). Regression equations – LMA y = -0.3228x + 35.415, R2 = 0.8576. CLAMP y = -0.1412x + 23.109, R2 = 0.8515.

80x75mm (300 x 300 DPI)

TABLE 1

Morphotype / systematic affinity	No. specimens	ML / SD (mm)	MW / SD (mm)	MQI
1 *Andromeda novaecaesarae* Hollick	2	33.4	9.9 / 0.7 (n = 2)	4
2 *Andromeda parlatorii* Heer	2	84.0* (n = 1)	36.0* (n = 1)	4
3 '*Aralia*' *groenlandica* Heer	9	57.0 / 1.4 (n = 2)	51.3 / 2.5 (n = 2)	5
4 *Araliopsoides cretacea* (Newberry) Berry	1	67.8	57.9	7
5 *Celastrophyllum albaedomus* Ward	6	54.0 (n = 1)	14.8 (n = 1)	4
6 *Celastrophyllum brittonianum* Hollick	2	30.6 (n = 1)	10.2 / 0.0 (n = 2)	7
7 *Cissites formosus* Heer	3	105.0* (n = 1)	95.0* (n = 1)	5
8 *Cissites platanoidea* Hollick	28	39.4 / 18.5 (n = 9)	41.0 / 19.8 (n = 10)	7
9 *Crassidenticulum* sp. indet	8	NA	NA	2
10 *Daphnophyllum dakotense* Lesquereux	1	53.3	17.6	2
11 '*Densinervum' kaulii* Upchurch & Dilcher	3	NA	NA	2
12 *Dicotylophyllum* sp. indet	2	39.4 / 0.6 (n = 2)	17.8 / 0.4 (n = 2)	5
13 *Diospyros primaeva* Heer	4	93.0* (n = 1)	29.0* (n = 1)	4
14 *Dryandroides lanceolata* Knowlton	1	91.0*	10.0*	5
15 *Dryandroides* sp. indet	2	NA	NA	4
16 *Ficus berthoudi* Lesquereux	10	89.0* (n = 1)	25.4 / 6.3 (n = 3)	4
17 *Liriodendron simplex* Newberry	2	23.8 (n = 1)	14.0 (n = 1)	4
18 *Liriodendropsis simplex* Newberry	9	31.1 / 13.9 (n = 4)	16.0 / 7.6 (n = 5)	6
19 *Magnolia amplifolia* Heer, *Magnolia speciosa* Heer	13	96.1 / 17.3 (n = 4)	46.6 / 9.2 (n = 4)	6
20 *Magnolia* sp. indet	4	NA	46.3 / 12.8 (n = 3)	4
21 *Menispermites obtusiloba* Lesquereux	1	58.5	61.6	5

22 *Menispermites trilobatus* Berry	2	71.0* (n = 1)	69.0* (n = 1)	3
23 *Platanus heerii* Lesquereux	3	NA	NA	5
24 *Platanus shirleyensis* Berry	3	78.5 / 54.5 (n = 2)	42.9 / 18.1 (n = 3)	7
25 *Salix newberryana*	2	5.2 / 29.2 (n = 2)	6.0 / 0.6 (n = 2)	3
26 *Sassafras acutilobum* Lesquereux	23	54.9 / 7.7 (n = 3)	27.9 / 6.0 (n = 3)	6
27 '*Sterculia*' *lugubris* Lesquereux	1	NA	NA	4
28	1	NA	NA	3
29	3	NA	5.8 / 2.0 (n = 5)	4
30	1	47.4	54.7	4
31	5	NA	10.2 / 2.1 (n = 3)	3
32	1	51.0	45.0	5
33	2	NA	NA	2
34	1	NA	NA	4
35	3	33.1	41.3	5
36	2	NA	NA	4
37	1	NA	16.2	5
38	1	NA	22.3	5
39	1	NA	17.1	4
40	1	NA	NA	5
41	2	NA	NA	4
42	1	NA	NA	5
43	1	16.2	18.3	4
44	1	NA	NA	3
45	1	NA	NA	5
46	1	20.2	28.3	7
Total No. specimens	177	45	66	-

Abbreviations are as follows: mean length / standard deviation (ML / SD), mean width / standard deviation (MW / SD), and morphotype quality index (MQI) (see Harris & Arens, 2016 for details). NA indicated when data was unavailable for a measurement or a calculation. * Estimates from Armstrong (1993). More information on morphotype classification can be found in Demers-Potvin and Larsson (2019).

TABLE 2

Physiognomic Method Used	MAT (°C)	WMMT (°C)	CMMT (°C)	LGS (Months)	GSP (cm)	MMGSP (cm)
CLAMP (GRIDMet)	15.1 ± 2.1	23.1 ± 2.5	7.8 ± 3.4	8.4 ± 1.1	119.6 ± 31.7	13.6 ± 3.8
CLAMP (Met)	15.4 ± 2.0	23.9 ± 2.7	8.0 ± 3.4	10.7 ± 1.1	153.3 ± 48.3	16.1 ± 5.2
CLAMP (Global378)	13.5 ± 4.0	23.7 ± 3.9	3.4 ± 6.7	9.3 ± 1.9	86.7 ± 54.9	6.0 ± 6.0

Physiognomic Method Used	Three WET (cm)	Three DRY (cm)	RH (%)	SH (g/kg)	ENTHAL (kJ/kg)
CLAMP (GRIDMet)	68.1 ± 22.9	16.6 ± 5.9	71.9 ± 8.6	8.5 ± 1.7	32.1 ± 0.8
CLAMP (Met)	70.5 ± 20.6	27.1 ± 13.7	66.0 ± 11.1	7.4 ± 1.7	30.8 ± 0.6
CLAMP (Global378)	59.8 ± 32.2	7.2 ± 13.0	57.0 ± 9.3	7.4 ± 2.0	31.9 ± 1.1

For CLAMP, all errors are 2σ, and are calculated by treating samples from each modern calibration site as passive (retrieved from Spicer, 2006). 'GRIDMet' refers to estimates obtained from an analysis that uses a temperate North American gridded meteorological calibration dataset, 'Met' refers to estimates obtained from an analysis that uses an alternative ungridded North American calibration dataset, and 'Global378' refers to estimates obtained from an analysis that uses a more global gridded calibration dataset (see Spicer, 2006; Spicer et al., 2009 for more details). Abbreviations for the climate parameters are as follows: mean annual temperature (MAT), warmest month mean temperature (WMMT), coldest month mean temperature (CMMT), length of the growing season (LGS), growing season precipitation (GSP), mean monthly growing season precipitation (MMGSP), precipitation during three wettest months (Three WET), precipitation during three driest months (Three DRY), relative humidity (RH), specific humidity (SH), and enthalpy (ENTHAL). See Demers-Potvin and Larsson (2019) for CLAMP physiognomic character state frequencies in scoresheet.

TABLE 3

Flora (Formation)	P.Lat (°N) (Min; Max)	MAT reference	Method	MAT (°C) (SE)	WMMT (°C) (SE)	CMMT (°C) (SE)	LGS (Months) (SE)	GSP (cm) (SE)
Woodbridge (Raritan)	36.4 (33.2; 39.8)	Wolfe and Upchurch (1987)	LMA	26.0 (2.7)	-	-	-	-
South Amboy (Raritan)	36.4 (33.2; 39.8)	Wolfe and Upchurch (1987)	LMA	22.8 (4.4)	-	-	-	-
Milton (Raritan)	36.4 (33.2; 39.8)	Wolfe and Upchurch (1987)	LMA	23.9 (4.6)	-	-	-	-
Malden Mtn (Patapsco)	36.4 (33.2; 39.8)	Wolfe and Upchurch (1987)	LMA	23.6 (4.8)	-	-	-	-
Arthurs Bluff (Woodbine)	37.4 (30.7; 33.9)	Wolfe and Upchurch (1987)	LMA	26.5 (3.6)	-	-	-	-
Denton Co. (Woodbine)	37.4 (30.7; 33.9)	Wolfe and Upchurch (1987)	LMA	25.1 (3.0)	-	-	-	-
Fort Harker (Dakota)	39.0 (35.8; 42.5)	Wolfe and Upchurch (1987)	LMA	24.5 (3.9)	-	-	-	-
Dunvegan (Dunvegan)	58.4 (55.2; 61.8)	Wolfe and Upchurch (1987)	LMA	17.8 (4.2)	-	-	-	-
Chandler (Chandler)	78.0 (74.7; 81.3)	Parrish and Spicer (1988)	LMA	10.9 (3.3)	-	-	-	-
Redmond (Redmond)	48.8 (45.6; 52.2)	Hickey and Armstrong (1998)	LMA	19.9 (5.2)	-	-	-	-
		This study	CLAMP (G)	15.1 (2.1)	23.1 (2.5)	7.8 (3.4)	8.4 (1.1)	119.6 (31.7)
Rose Creek (Dakota)	40.2 (37.0; 43.6)	This study	CLAMP (G)	16.9 (2.1)	26.5 (2.5)	8.0 (3.4)	9.1 (1.1)	173.1 (3.8)
Fort Harker (Dakota)	39.0 (35.8; 42.5)	This study	CLAMP (G)	16.5 (2.1)	23.2 (2.5)	10.2 (3.4)	9.1 (1.1)	127.1 (3.8)
Tuscaloosa (Tuscaloosa)	31.7 (28.5; 35.1)	Spicer and Herman (2010)	CLAMP (G)	19.7 (2.1)	24.5 (2.5)	15.1 (3.4)	10.5 (1.1)	145.6 (3.8)

Woodbine (Woodbine)	37.4 (30.7; 33.9)	Spicer and Herman (2010)	CLAMP (G)	19.4 (2.1)	23.5 (2.5)	15.4 (3.4)	10.3 (1.1)	130.5 (3.8)
Nanushuk (Corwin)	79.5 (76.3; 82.9)	Herman *et al*. (2016)	CLAMP (G)	12.5 (2.1)	20.0 (2.5)	5.7 (3.8)	-	-

LMA standard errors retrieved from Miller *et al*. (2006: equation (3)). CLAMP (G) refers to estimates calibrated with global gridded climate data using the methodology of Spicer *et al.* (2009). All CLAMP errors are 2σ, and are calculated by treating samples from each modern calibration site as passive (retrieved from Spicer, 2006). Abbreviations for the climate parameters are as follows: palaeolatitude (P.Lat), mean annual temperature (MAT), warmest month mean temperature (WMMT), coldest month mean temperature (CMMT), length of the growing season (LGS), and growing season precipitation (GSP). Palaeolatitudes calculated on www.paleolatitude.org (model version 2.1) using the reference frame of Torsvik *et al*. (2012); for more details on the calculator, see Hinsbergen *et al*. (2015). See Demers-Potvin and Larsson (2019) for CLAMP physiognomic character state frequencies in scoresheets.